NSEL Report Series
Report No. NSEL-026
October 2010

Nonlinear Behavior of Controlled Rocking Steel-Framed Building Systems with Replaceable Energy Dissipating Fuses

Kerry S. Hall,
Matthew R. Eatherton,
Jerome F. Hajjar

NEWMARK STRUCTURAL ENGINEERING LABORATORY

Department of Civil and Environmental Engineering
University of Illinois at Urbana-Champaign

UILU-ENG-2010-1805

ISSN: 1940-9826

The Newmark Structural Engineering Laboratory (NSEL) of the Department of Civil and Environmental Engineering at the University of Illinois at Urbana-Champaign has a long history of excellence in research and education that has contributed greatly to the state-of-the-art in civil engineering. Completed in 1967 and extended in 1971, the structural testing area of the laboratory has a versatile strong-floor/wall and a three-story clear height that can be used to carry out a wide range of tests of building materials, models, and structural systems. The laboratory is named for Dr. Nathan M. Newmark, an internationally known educator and engineer, who was the Head of the Department of Civil Engineering at the University of Illinois [1956-73] and the Chair of the Digital Computing Laboratory [1947-57]. He developed simple, yet powerful and widely used, methods for analyzing complex structures and assemblages subjected to a variety of static, dynamic, blast, and earthquake loadings. Dr. Newmark received numerous honors and awards for his achievements, including the prestigious National Medal of Science awarded in 1968 by President Lyndon B. Johnson. He was also one of the founding members of the National Academy of Engineering.

Contact:
Prof. B.F. Spencer, Jr.
Director, Newmark Structural Engineering Laboratory
2213 NCEL, MC-250
205 North Mathews Ave.
Urbana, IL 61801
Telephone (217) 333-8630
E-mail: bfs@uiuc.edu

This research was funded by the National Science Foundation (Grant No. CMS-0530756), by a University of Illinois Fellowship, and by the University of Illinois at Urbana-Champaign. The authors thank the following for their assistance with this research: Prof. Gregory G. Deierlein, principal investigator on the project, Profs. Helmut Krawinkler and Sarah Billington, co-principal investigators on the project, Dr. Paul Cordova, Mr. Eric Borchers, and Mr. Xiang Ma, all from Stanford University, Stanford, California; and Mr. David Mar, Tipping-Mar and Associates, Berkeley, California. Any opinions, findings, and conclusions or recommendations expressed in this material are those of the authors and do not reflect the views of the National Science Foundation.

The cover photographs are used with permission. The Trans-Alaska Pipeline photograph was provided by Terra Galleria Photography (http://www.terragalleria.com/).

ABSTRACT

This report summarizes the results of a parametric study of a controlled rocking seismic lateral resistance system that includes two steel braced frames linked by replaceable energy dissipating fuses that are engaged by controlled rocking behavior. The frames are post-tensioned vertically to the foundation so as to facilitate self-centering after rocking. The study was conducted using geometrically and materially nonlinear finite element analysis of a two-dimensional prototype of the structural system. In this study, the structure is subjected to a suite of far-field ground motions representing different hazard levels in the Western U.S. The characteristics of the structural fuses, which absorb energy through a combination of cyclic shear and localized flexure mechanisms, were based on experimental test results of steel slit shear panels and engineered cementitious composite shear panels. Three key parameters are investigated that affect the response. The first is the ratio, A/B, of the bay width of the braced frames as compared to the width of the shear fuses connecting the frames. The second is the overturning factor (OT), which is the ratio of the total resisting moment of the fuses and post-tensioning compared to the overturning forces in the design code. The third is the self-centering factor (SC), which is the ratio of restoring moment of PT to the resisting moment of the fuses. Based on the computational results, recommendations are made for appropriate ranges of values for each of these parameters for effective performance.

CONTENTS

INTRODUCTION

A new structural system is explored in this research which seeks to minimize widespread structural damage in the lateral-resisting system by using a controlled-rocking system, with vertical post-tensioning used to enable self-centering, and the concept of replaceable energy-dissipating fuses for ease of repair. To understand this system, each of these components of the system is explored in this work through a series of parametric studies that document the seismic response of a prototype structural system. A prototype structure for this system is analyzed using a series of 23 ground motions to assess the sensitivity of response to the variation of each key parameter in the system that relates to the controlled rocking response. At the end of the report, a summary of the system response is provided to facilitate future research on this system.

1.1 Performance of Rocking Systems

Rocking has been explored as a means of reducing seismic damage from strong earthquakes (e.g., Azuhata et al. 2003, Ajrab et al. 2004, Chen et al. 2006, Toranzo et al. 2001). The rocking mechanism can filter out earthquake energy, providing some seismic isolation and reducing the maximum base shear (Meek 1975). This can substantially lower foundation costs by reducing the moment that piles must resist to prevent uplift (Makris and Konstantinidis 2003). The response of free rocking systems is nonlinear and potentially sensitive to small changes in the aspect ratio. In slender structures, overturning may also occur. Rocking resistance and safety against overturning can be improved by anchoring the structure with prestressed tendons (Aslam et al. 1980).

1.2 Self-centering Systems

Residual deformations after moderate to large earthquakes can render a building nearly irreparable even though it survives the ground motion. Some researchers have been exploring the use of post-tensioned cables (PT) to provide a restoring force in structures (e.g., Pekcan et al. 2000, Christopoulos et al. 2002, Wolski et al. 2006, Sause et al. 2006). These systems give the frames a tendency to self-center even after large displacements and nonlinear energy dissipating damage. Systems that self-center can be repaired more economically.

A secondary goal of these systems is to dissipate energy thereby reducing the displacements under seismic loading. To achieve both of restoring force and energy dissipation researchers develop systems with flag-shaped hysteresis loops as in Figure 1. Passing through zero on the return curve signifies self-centering. The area under the hysteresis curve signifies the energy dissipated. The area is enlarged by allowing part of the structure to deform inelastically, but at a strength less than the restoring force of the post-tensioning so that the system is able to self-center (Christopoulos et al. 2002).

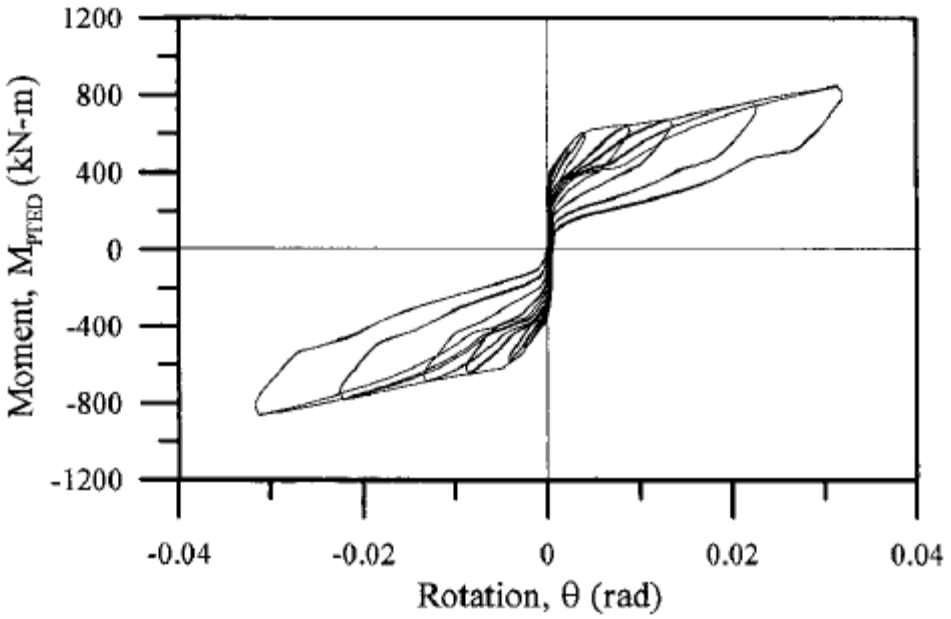

Figure 1 – Flag-Shaped Hysteresis Example

1.3 Shear Panel Experiments

To dissipate seismic energy and assure ease of repair after a damaging earthquake, modular shear panels will be used as fuses in the lateral resisting system. During maximum considered event these shear panels may undergo shear deformations as large as 7-12% strain depending on the geometry of the system. To achieve the large shear deformations, very ductile innovative shear panel systems must be explored.

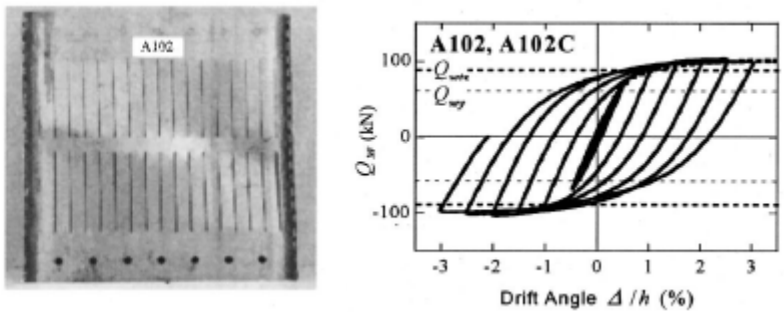

Figure 2 – Slotted Steel Shear Wall Tests

Some tests have been performed on steel shear walls with slits added to increase the energy dissipation and deformation capacity by creating the effect of many shallow link beams (Hitaka and Matsui 2003). In these experiments only tested the panels to 3% strain, but at that level several of the tests showed little or no degradation or softening and very good energy dissipation (Figure 2). Further investigation of these panels is ongoing at Stanford. ABAQUS analyses show that the panels may sustain strains up to strains of 10% (Figure 3).

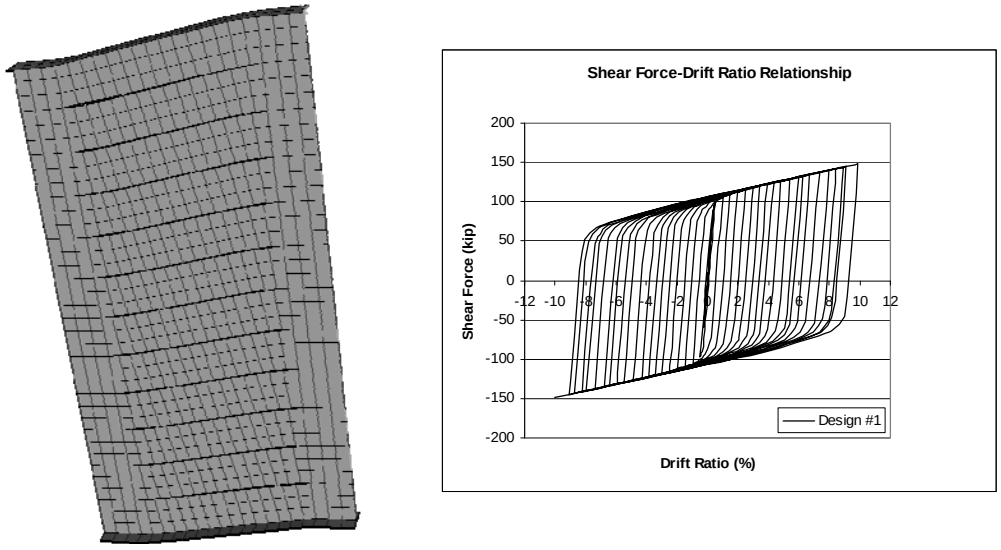

Figure 3 – ABAQUS Analysis of Slotted Shear Panel

Coupling beams precast with high-performance fiber-reinforced cement composites (HPFRCC) have shown promise for achieving high shear strains (Canbolat et al. 2005). The HPFRCC mixes have high tensile strength and moderate ductility due to gradual yielding of the steel fibers as they are pulled out. In experiments one coupling beam specimen was loaded up to 4% strain cyclically and then monotonically displaced up to nearly 8% (Figure 4).

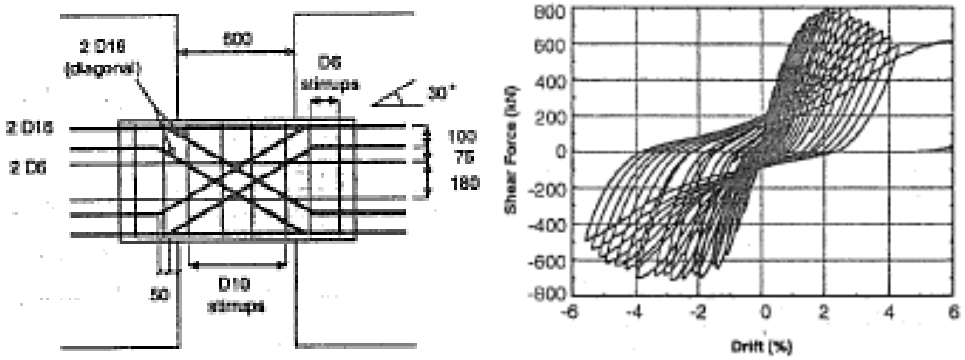

Figure 4 – HPFRCC Coupling Beam Test

Another series of experimental concrete mixes referred to as engineered cementitious composites (ECC) uses coated PVA fibers in a carefully designed cement matrix to achieve higher material ductility (Li et al. 1994). In a shear panel test with this material using minimal reinforcement, the specimen was loaded up 6% strain and showed strain hardening behavior until just before failure (Figure 5). With additional reinforcement these panels may be a viable option for shear fuses. Further testing of both HPFRCC and ECC panels for use as replaceable shear fuses is ongoing at Stanford.

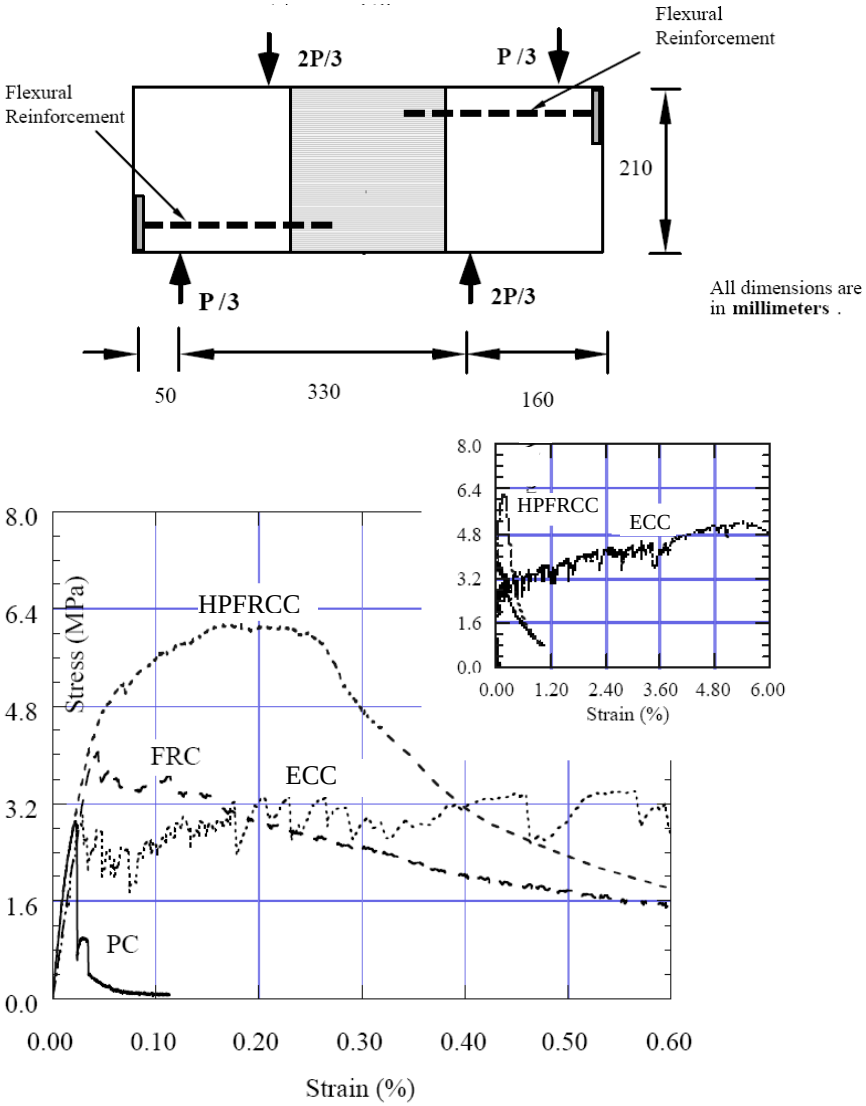

Figure 5 – ECC Shear Panel Test

PROTOTYPE DESIGN

The proposed system consists of two steel braced frames which are free to uplift from their foundations (Figure 6). In order to allow uplift and rocking while transferring shear, a trough foundation detail was developed. The base of the frame is not fastened to the foundation, but the walls of the trough prevent the base from displacing excessively and allow transfer of base shear in compression. The frames are connected to the gravity framing system by shear tabs which can be idealized as pins. The two frames are post-tensioned vertically by high strength steel strands in the middle of each frame. Positioning the PT mid-frame rather than at the columns reduces the strain demand on the cables at a given uplift by a factor of 2. This is important in low rise buildings to prevent yielding of the PT. The shear panels are fastened between the frames. By positioning the fuses in the center and allowing both frames to uplift, the strain in the fuse is doubled. This concentrates damage at the fuse, simplifying system repair after an earthquake.

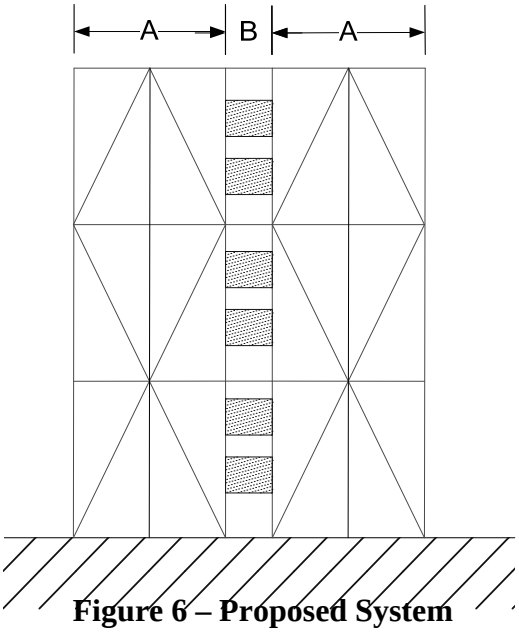

Figure 6 – Proposed System

The centerline width of each frame will be referred to as A and the centerline width of the fuse space between them will be referred to as B. The ratio of A/B determines the relationship between frame drift and shear panel strain. The smaller A/B ratios result in lower fuse strains.

To calculate the desired strength of the PT and fuses two controlling factors have been defined, the overturning factor and the self-centering factor. The overturning factor (OT) pertains to the total resisting moment of the fuses and post-tensioning compared to the overturning forces in the design code. The OT is inversely related to the *R* factor in design codes. An OT of 1 relates to an *R* of 8, while an OT of 2 is equivalent to changing the *R* to 4. The self-centering factor (SC) is the ratio of restoring moment of PT to

resisting moment of the fuses. SC directly affects the residual drifts. High SC ensures low residuals.

$$OT = \frac{M_{resist}}{M_{OVT}} = \frac{A F_{PT} + V_P (A+B)}{M_{OVT}} \qquad SC = \frac{A F_{PT}}{V_P (A+B)}$$

where: A = Center-to-center distance of the columns in each individual frame
B = Center-to-center distance between the columns on each side of the fuse
F_{PT} = Initial axial tension force in the PT
V_P = Shear strength of the fuse
M_{OVT} = Overturning moment due to static code loading

The overturning moment is calculated from the ASCE 7-05 equivalent lateral loads. To calculate the fuse strength and PT used in each model, the two equations shown above are solved simultaneously. To increase OT but hold SC constant, the fuse and PT strengths are increased proportionally. To increase SC and hold OT constant, the fuse strength is reduced while the PT is increased.

The fuse and PT must also be checked for global overturning, which occurs when the fuse overcomes the PT lifting one of the frames completely off of the foundation (Figure 7). Global overturning can be prevented by satisfying the equation $F_{PT} > V_P$.

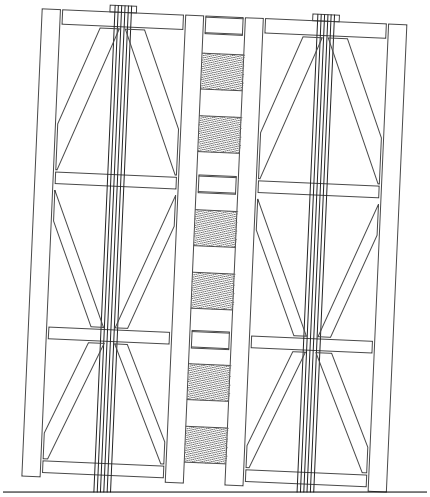

Figure 7 – Global Overturning

As part of the SAC Joint Venture, a standard office building was designed for comparison of seismic designs (Gupta and Krawinkler 1999). Floor plans, elevations, and loadings were specified for 3, 9, and 20-story buildings (Figure 8). The 3-story SAC building was chosen as the prototype structure for the study of the controlled rocking system. The system was designed for two sets of rocking frames in each direction on the perimeter.

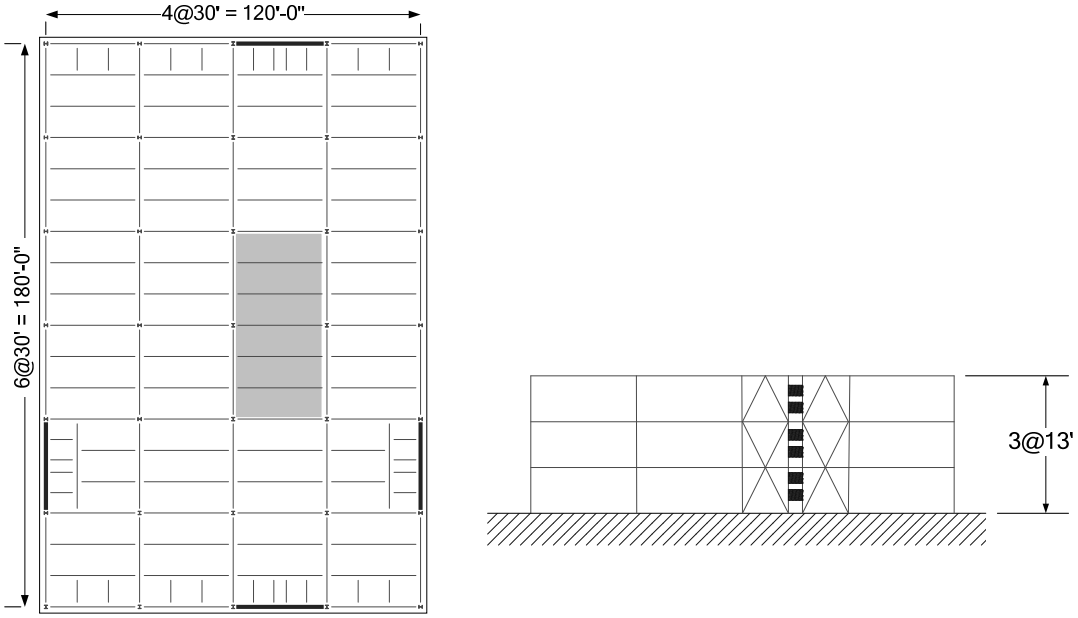

Figure 8 – SAC 3-story Building

From the masses and loadings specified for the SAC building the following masses and loads were calculated.

Table 1 - Prototype Loads

	Seismic Mass	Floor Dead Load	Wall Dead Load	Floor Live Load
Roof	1.033 kN-s^2/mm	9459 kN	684 kN	1974 kN
Floors 2 and 3	0.955 kN-s^2/mm	9474 kN	890 kN	1974 kN

The sizing of the frame members was done based on a simple static analysis using a triangular lateral load distribution and the full capacity of the fuse and PT to determine the member forces. The girders are W12x30 in each story; the column sizes are W12x120 in the outer columns, W12x79 in the inner columns; the braces are W12x79 in the first story, W12x72 in the second, and W12x96 in the third story.

COMPUTATIONAL MODEL DEVELOPMENT

A model was developed in OpenSEES to accurately represent the system. Geometric nonlinearity due to large displacements and unusual boundary conditions were cause for concern. Careful consideration went into the modeling of every detail. Figure 9 shows the finite element mesh and boundary conditions used for these analyses.

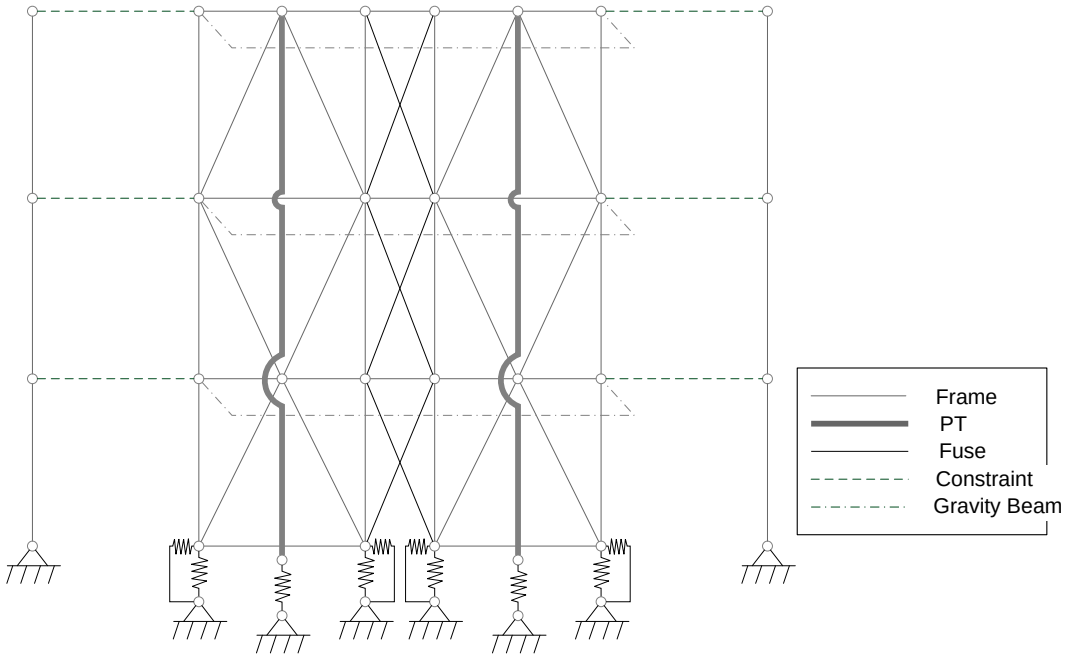

Figure 9 – Diagram of OpenSees Model

To allow rocking, the vertical restraint of the frame's base nodes was modeled using a no-tension elastic constitutive relationship. A duplicate node was placed at each base node and fixed in place. Zero length elements with a no-tension constitutive relationship were used to connect the nodes with a vertical orientation. By making the compression stiffness of these gap elements very high, the effective behavior is free uplift but solid restraint downward.

Regarding transferring the base shear, because of the geometric nonlinearity of the system, if both frame base nodes were constrained to have zero horizontal displacement the frame would be over-constrained. During rocking the uplifted frame base rotates about the pivoting node. If the uplifted node is not free to translate horizontally it partially restrains the rocking. For this reason it was decided that only the pivot node should transfer shear. This was achieved using gap elements oriented horizontally in opposite directions. The result is that the right base node of the frame transfers base shears only to the right and the left node only to the left. This matches very well with the trough base detail which has been developed.

Because the frame was designed to remain elastic, a simple elastic constitutive model was used for the frame members. The flexural stiffness of the beams and columns had little effect on system response since the frame is well braced. After this was confirmed by a study performed with pushover analysis, all frame members were modeled using four degree of freedom corotational truss elements. The corotational elements are formulated to be accurate with large displacements.

The post-tensioning was also modeled using corotational truss elements. A strain-hardening constitutive relationship was used for the cables, yielding at 85% of the guaranteed ultimate tensile strength and hardening to reach the ultimate strength at the rupture strain (Figure 10). The prestressing of the post-tensioning system was achieved by shifting the constitutive relationship of the cables to the left. This results in an initial stress at zero strain. Because the flexibility of the frame relieves some of the stress, an adjustment factor was determined iteratively. To prevent the cables from going into compression when the system is centered after the steel has yielded, gap elements were once again employed with their orientations reversed so that they provided a zero-compression behavior with very high tensile stiffness. This constraint allows the cable to effectively go limp if it is put into compression and not reverse any yielding that has taken place.

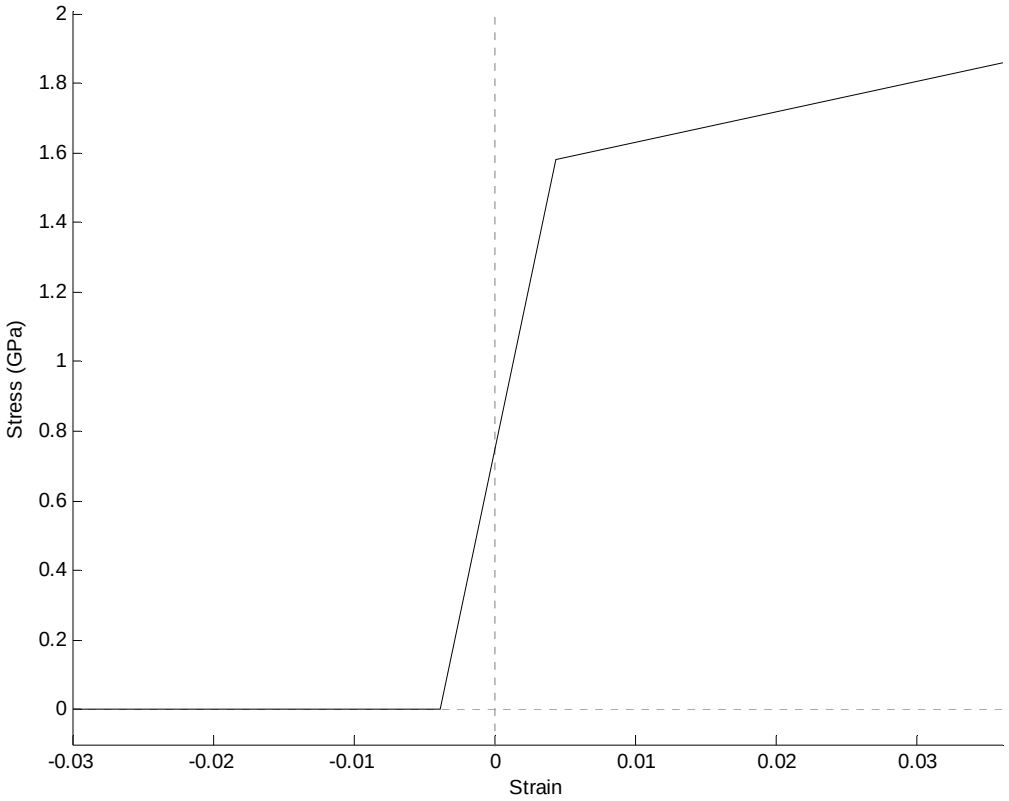

Figure 10 – PT Cable Constitutive Relationship

Because OpenSees lacks hysteretic relationships for its quad elements, the fuses were modeled by equivalent truss elements in the form of cross-bracing at each floor. The area, stiffness, and strength of these truss elements were calculated to match the

desired response of the shear panels. The constitutive relationships of these truss elements were tailored to achieve the different constitutive relationships of slotted steel and cementitious composite fuses. Elastic-perfectly plastic and degrading-pinching constitutive models available for axial elements in OpenSees accurately captured the shear panels' complex constitutive relationships, further described in section 4.4. To account for the effective fuse width, the stiffness of each fuse was input in units of kN/mm and the yield strain of the fuse was calculated from the member centerline width of the fuse. In post-processing the strains calculated from the nodal displacements were adjusted by multiplying by the centerline width and dividing by the effective width between the panel connections.

To prevent stress demands on the fuses from the transfer of lateral load between the two frames, link beams were placed between the frames at each story level. These links were assigned an area equal to that of the beams in the rocking frames, but given constitutive properties which allow them to yield so that they would not become an unrealistic locking mechanism at large rocking drifts.

Since vertical restraint between the interior columns and the gravity system would impose the large shear forces of the fuse on the slab, it was assumed that these columns would be isolated from the slab by a separate beam. It was also assumed that a connection flexible in the vertical direction but stiff laterally would be made between this gravity beam and the interior columns to brace and transmit horizontal forces into the system. The gravity load and vertical mass directly tributary to the system were therefore applied only at the outer columns while the horizontal mass was distributed evenly between all four columns.

To model the effects of the gravity framing system on the spacing of the rocking frames, another truss element was placed between the outer columns at each floor level. This element was assigned an area equal to a beam carrying the gravity load in parallel with the system. This element restrains the contraction of the outer columns of the system, affecting the rocking behavior of the two frames.

Leaning columns were modeled to simulate the effect of the gravity frame to prevent self-centering. These leaning columns consisted of a three link assembly constrained at each floor to move equally with the outer columns of the frame in the horizontal direction. The gravity load of the rest of half of the building was put on these columns so that when the building deforms horizontally it causes a horizontal reaction increasing the lateral load on the system. This is a reasonable representation of what happens in a real building.

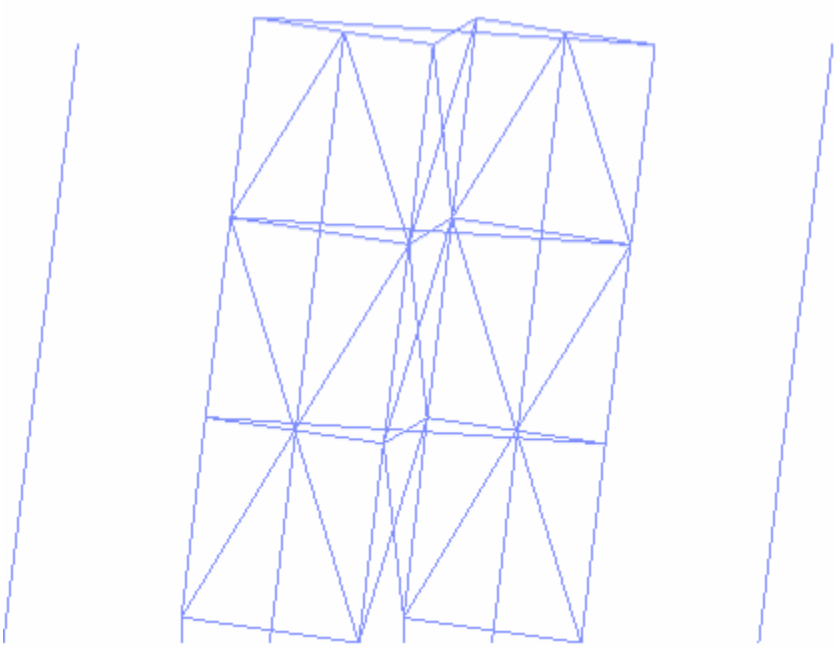

Figure 11 – OpenSees Model Rocked Configuration

PARAMETRIC STUDY

A parametric study was conducted to determine the significance of the A/B ratio, overturning factor (OT), and self-centering factor (SC) on the three-story prototype controlled rocking system. Pushover analyses were carried out for each configuration and eigenvalues were found at each load step. Time history analyses were also run with a suite of ground motions at multiple hazard levels to access the response of the system.

The fuse type was held constant through the first three studies. A slotted steel fuse (Figure 12) with a thickness of 16mm, link height-to-thickness ratio (b/t) equal to 8.0, and one row of slots was used. Elastic-perfectly-plastic behavior was assumed. The effective fuse width, B_{eff}, was taken as B – 300mm to account for the 150mm angle connections on either side. The slot length, l, was taken as B_{eff} – 2*b to allow a separation between the damage at the end of the links and the connection to the column, thereby avoiding connection failure. The panel stiffness and strength were calculated using the equations from Hitaka et al. (2003). Strength was varied to achieve different OT factors and SC factors by adjusting the height of the fuse. A check was put in place to ensure that no fuse taller than the height of the building was used. Odd decimal fuse heights were allowed so that OT and SC values would be exact. The fuses for the fourth study are described in section 4.4.

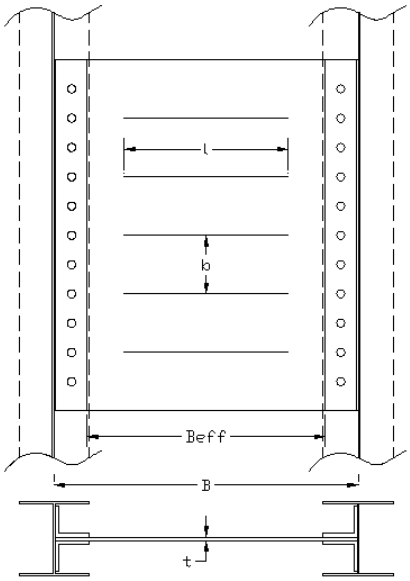

Figure 12 – Fuse Dimensions

The cyclic pushover analyses were conducted by displacing the roof of the frame by a given displacement to the right, and then displacing it by the same distance to the left. For clear graphic display, only two loading levels (+/- 1.25% and 2.5% drift) were applied. For the time history analyses, ground motion records were selected from the set of 40 proposed by Medina et al. (2004). These are shown in Appendix A. The records

and their response spectrums were acquired from the PEER strong motion database (2000). Each record was scaled so that its spectral acceleration at 1.0 seconds matched 0.26g, 0.6g, and 0.9g. These peak accelerations coincide with the 50% in 50, 10% in 50, and 2% in 50 occurrence probability, respectively, calculated from FEMA 356 and ASCE 7-05. Records requiring a scale factor greater than 4 to reach the 10% in 50 occurrence probability were rejected. Response spectra for the selected records are shown in Figure 13.

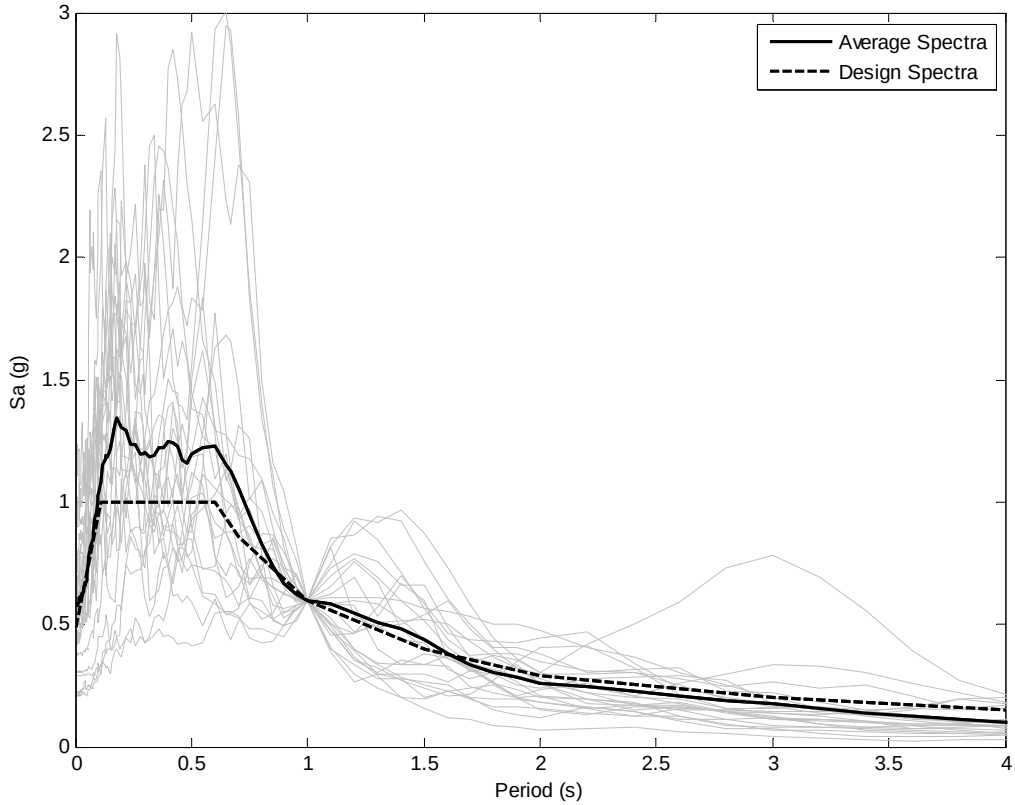

Figure 13 – Scaled Response Spectra for 10/50 Hazard

The range of variation for each parameter was chosen carefully. The A/B ratio was varied from 1.5 to 3, because lower A/B ratios lead to impractically steep chevron bracing and higher ratios cause shear strains that cannot be sustained by any of the fuses under current consideration. The bay spacing on each frame, center-to-center of the columns, is varied as part of the A/B ratio, but the total from outer column of each braced frame is held constant at 9 meters. The range of OT ratios considered was from 0.75 to 2.0. This corresponds to *R* values of 4 to 10.67. The lower OT limit was chosen to explore how the system would perform with an *R* greater than the maximum of 8 prescribed by the code. The upper limit was set because *R* values below 4 are generally undesirable in seismic design. The SC ratio was varied from 0.5 to 2.0 to explore the effect of this parameter on the residual drifts. The SC of 0.5, which permits global overturning, allowed the impact of that behavior to be observed. In the fuse study the

constitutive behavior of the fuse was varied between the elastic-perfectly plastic hysteretic used in the other studies and some pinching and degrading hysteretics.

Table 2 shows the parametric values of the analyses run in this study, along with the initial first mode period for the corresponding finite element model. The initial periods of all 13 configurations considered here were within 20% of each other (0.56 to 0.67 seconds). As the analyses proceed, there are multiple jumps in the tangent stiffness and thus in the first mode period that correspond to major changes in the stiffness of the system. The initial jump at approximately 0.1% roof drift occurs when the frames first uplift. The next jump in period occurs when the fuses start to yield. This happens at roof drift ratios between 0.3% and 0.5%. In some cases three discrete jumps can be seen as each of the three fuses yield. Between 0.5% and 3% drift, the system undergoes some stiffening as the post-tensioning picks up additional tension; this region is marked by a decrease in the first mode period. Finally at approximately 3% drift the post-tensioning starts to yield. After the post-tensioning in both frames yields, the eigenvalues calculated for the system become negative and were therefore not shown in the graphs.

The legends in the following figures are labeled with parameters in the order A/B.OT.SC.Fuse. In the legend nomenclature each parameter was multiplied by 100 to eliminate decimal points. The cyclic pushover plots are also labeled with dissipated energy which was calculated stepwise as the net work of the pushover force at each level multiplied by the incremental distance displaced during that step. In the IDA plots, the median of the peak response values for each model are plotted as well as the median plus one standard deviation. Black markers represent median peak response values, while grey markers represent one standard deviation above median peak response. The median and standard deviation were calculated using standard statistical methods and not log-normal measures.

Table 2 - Analyses Included in Parametric Study

Analysis Index	A/B	OT	SC	Fuse #	A (m)	B (m)	F_{PT} (kN)	V_P (kN)	K_{Fuse} (kN/mm)	Initial first Mode Period, T_1 (sec)
1	1.5	1	1	1	3.38	2.25	2528	1517	69	0.67
2	2	1	1	1	3.6	1.8	2370	1580	122	0.63
3	2.5	1	1	1	3.75	1.5	2276	1625	196	0.60
4	3	1	1	1	3.86	1.29	2212	1659	295	0.58
5	2.3	0.75	1	1	3.7	1.6	1731	1207	123	0.63
6	2.3	1	1	1	3.7	1.6	2309	1609	164	0.61
7	2.3	1.25	1	1	3.7	1.6	2886	2011	205	0.60
8	2.3	1.5	1	1	3.7	1.6	3463	2414	246	0.59
9	2.3	2	1	1	3.7	1.6	4617	3218	327	0.56
10	2.3	1	0.5	1	3.7	1.6	1539	2145	218	0.59
11	2.3	1	0.75	1	3.7	1.6	1979	1839	187	0.60
12	2.3	1	1.5	1	3.7	1.6	2770	1287	131	0.62
13	2.3	1	2	1	3.7	1.6	3078	1073	109	0.63
14	2.3	1	1	2	3.7	1.6	2309	1609	164	0.61
15	2.3	1	1	3	3.7	1.6	2309	1609	164	0.61

4.1 A/B Ratio

The A/B ratio study shows relatively minor changes in all response values except fuse shear strains. The cyclic pushover curves for lower A/B ratios exhibit slightly softened behavior with less energy dissipation (see Figure 14). Period changes (Figure 15) are minor between the different A/B ratios. Peak roof drifts (Figure 16) and uplifts (Figure 17) exhibit only small differences with the lower displacements associated with the lower A/B ratios. The peak base shears also showed little variation with A/B (Figure 18). The vertical reactions at the base of each column were recorded and the maximum peak of these values was reported (Figure 19). These values signify the amount of force that must be transferred vertically through the frame. The vertical reactions are highest for the low A/B ratios since they require a higher proportion of PT force to achieve the same restoring force due to the decreased lever arm (A/2). There was no strong trend in the variation of accelerations with A/B. Peak horizontal accelerations (Figure 21) were nearly twice as high as the target S_a values from the ground motion scaling, and peak vertical accelerations (Figure 20) were approximately 3 times higher than the corresponding horizontal accelerations. The most notable and expected difference was in the fuse shear strain demands (Figure 22). The shears strains increased as the A/B ratio was increased. With variation in A/B from 1.5 to 3, the median peak strains increased by approximately 50%. The median peak strain for the A/B of 3 was approximately 13%. Residual displacements increased with decreasing A/B ratios. Median residual roof drifts (Figure

23) were less than 0.1% for the 2/50 hazard level and residual uplifts (Figure 24) were less than 1mm.

These results show that the reduction of the A/B ratio may be used to decrease fuse shear strains, keeping in mind that this will result in steeper bracing in the braced frames. Other quantities changed only slightly.

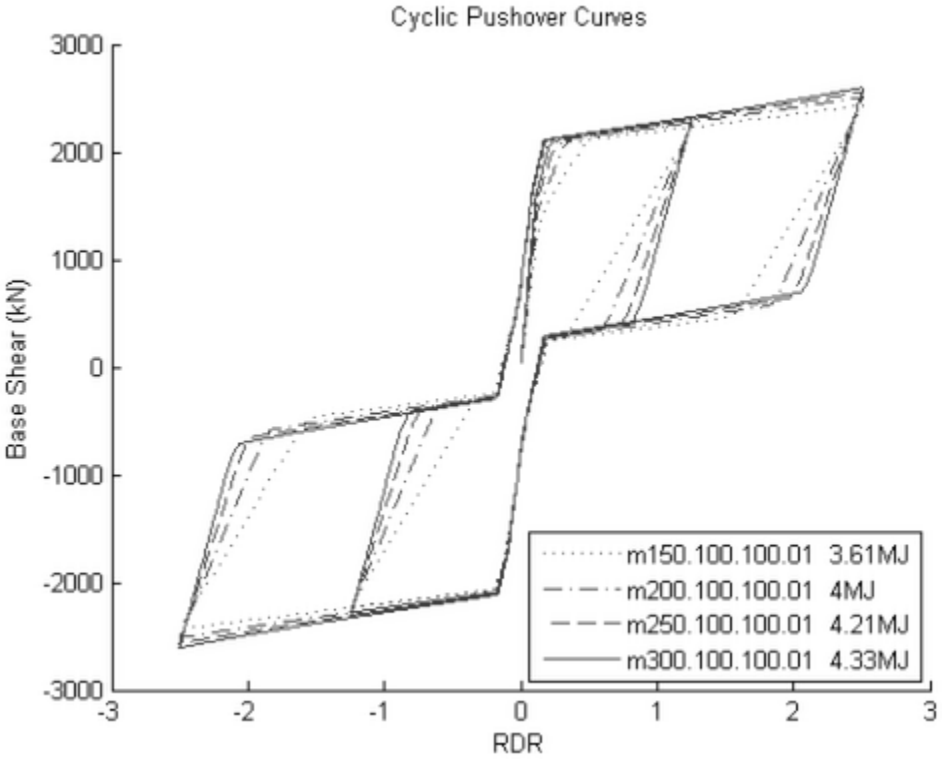

Figure 14 – A/B Study Cyclic Pushover Comparison

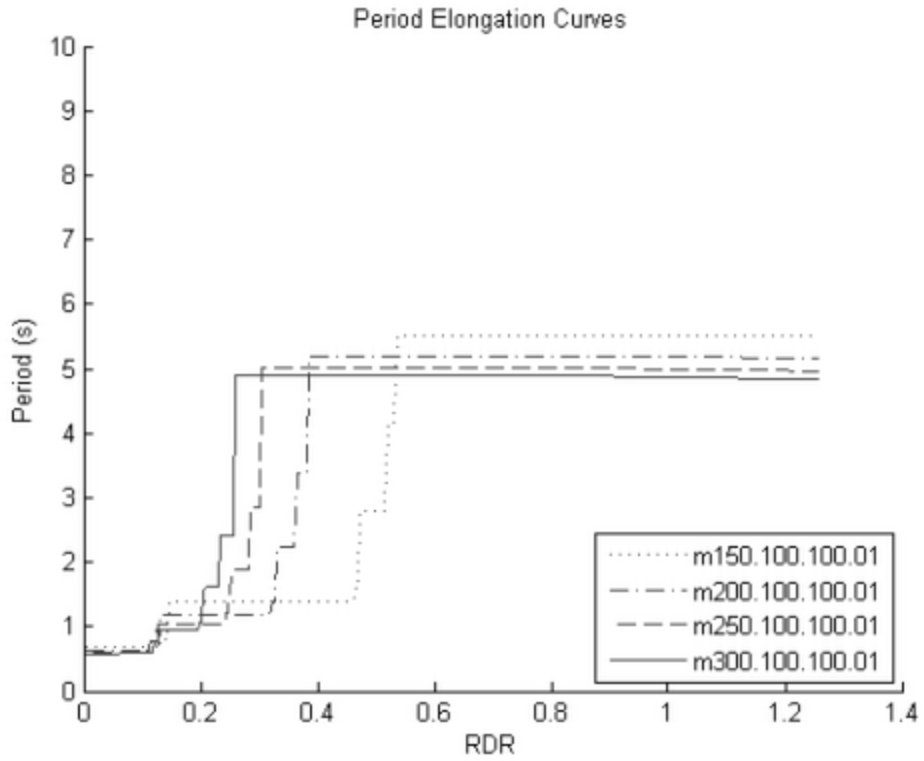

Figure 15 – A/B Study Period During Pushover

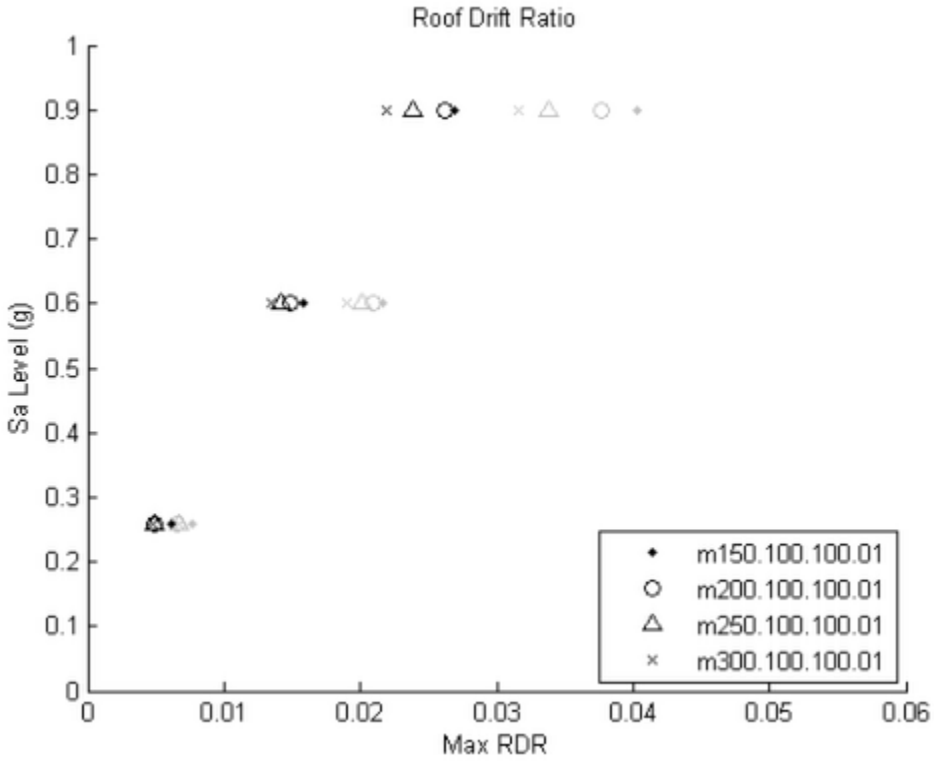

Figure 16 – A/B Study Peak Roof Drift Ratio Comparison

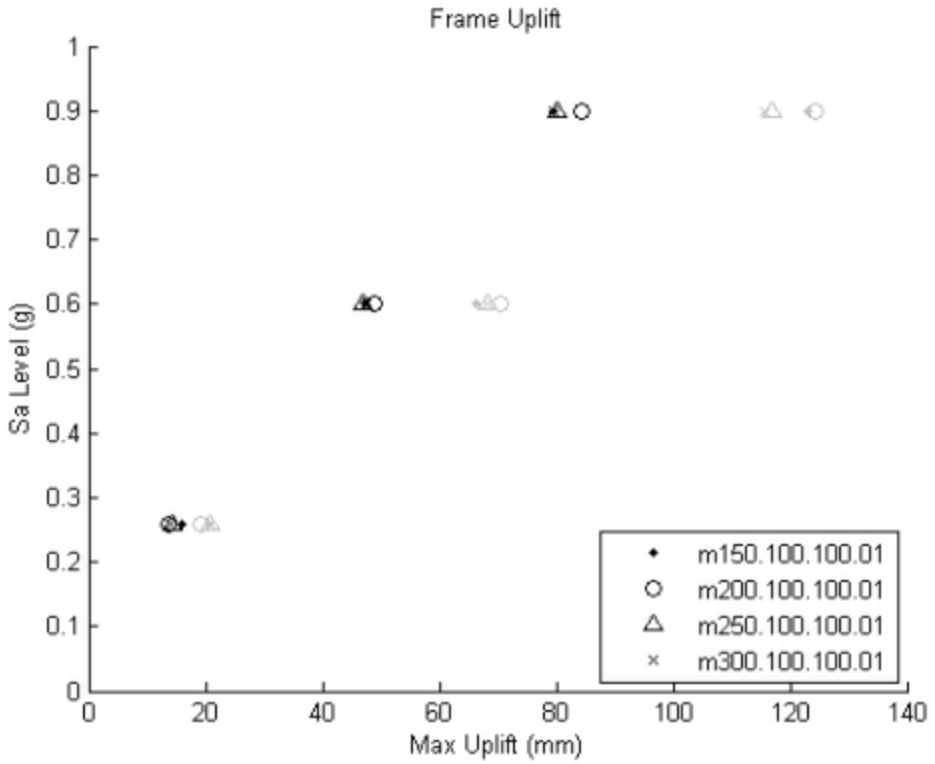

Figure 17 – A/B Study Peak Uplift Comparison

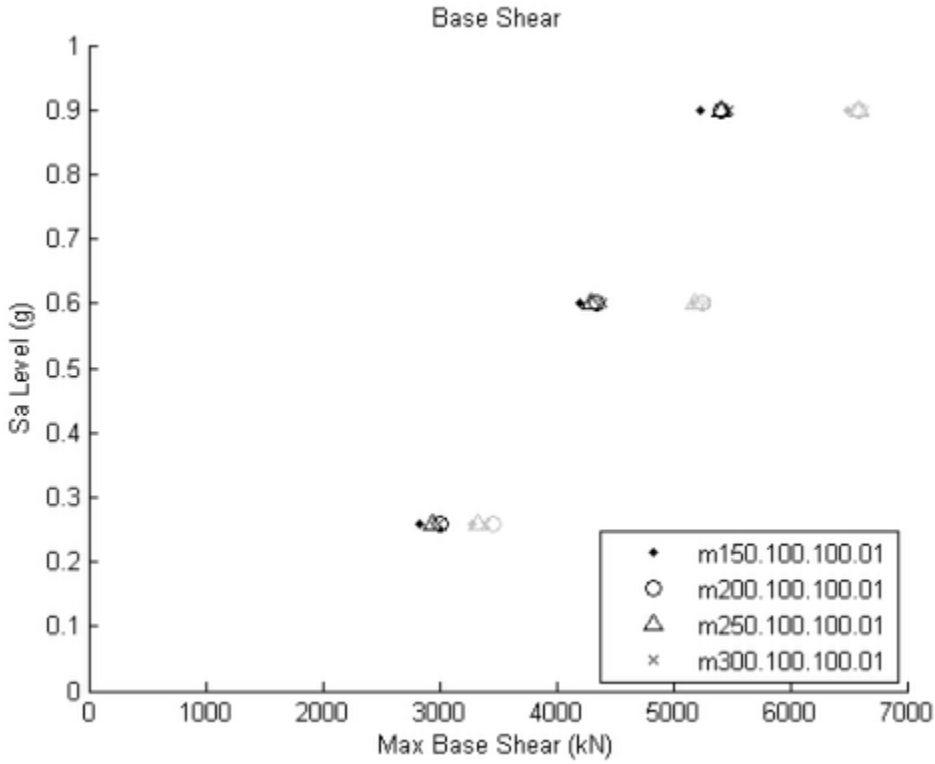

Figure 18 – A/B Study Peak Base Shear Comparison

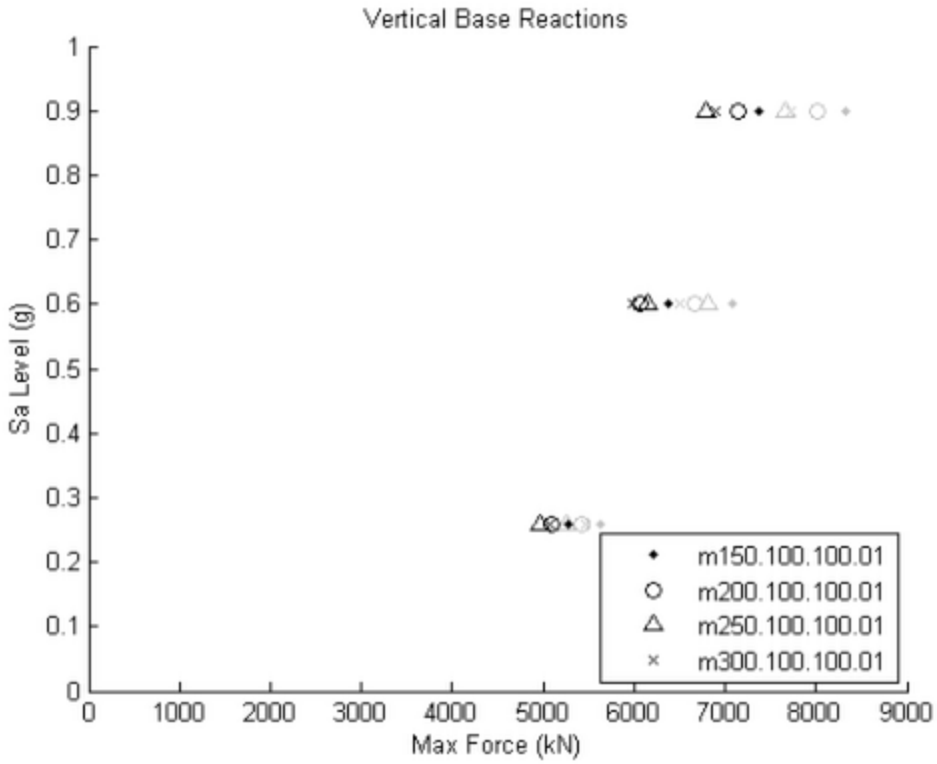

Figure 19 – A/B Study Peak Vertical Base Reactions Comparison

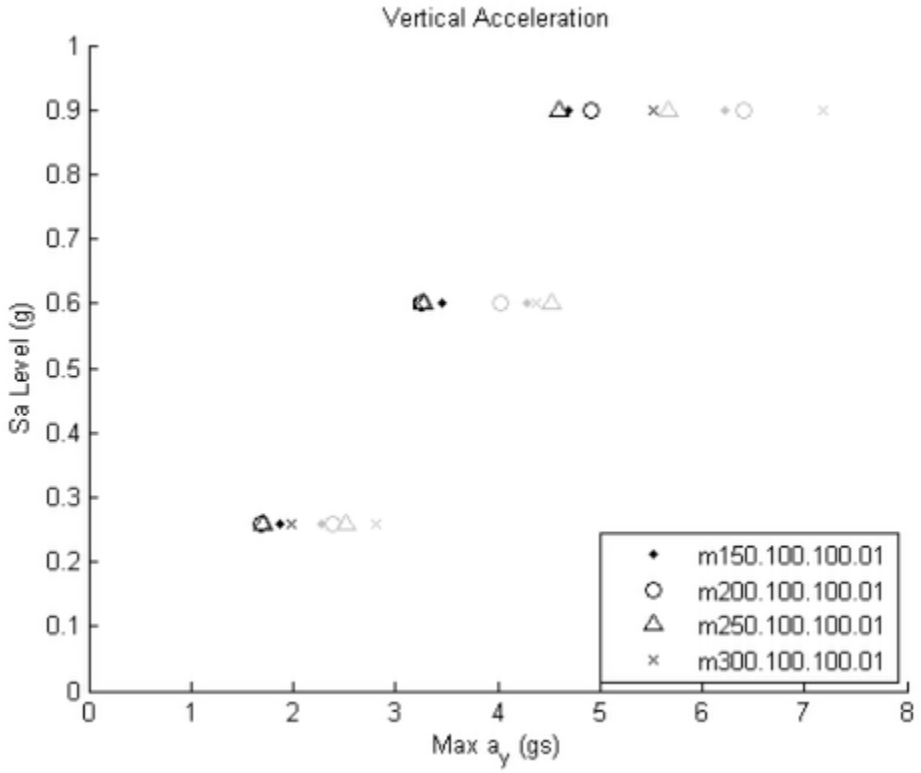

Figure 20 – A/B Study Peak Vertical Acceleration Comparison

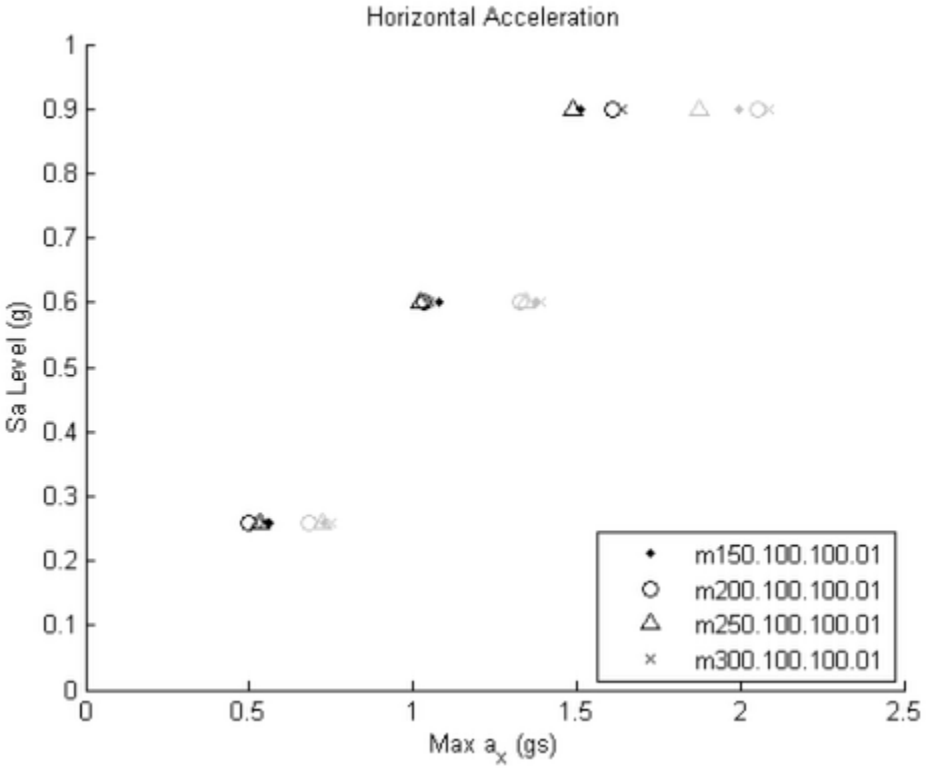

Figure 21 – A/B Study Peak Horizontal Acceleration Comparison

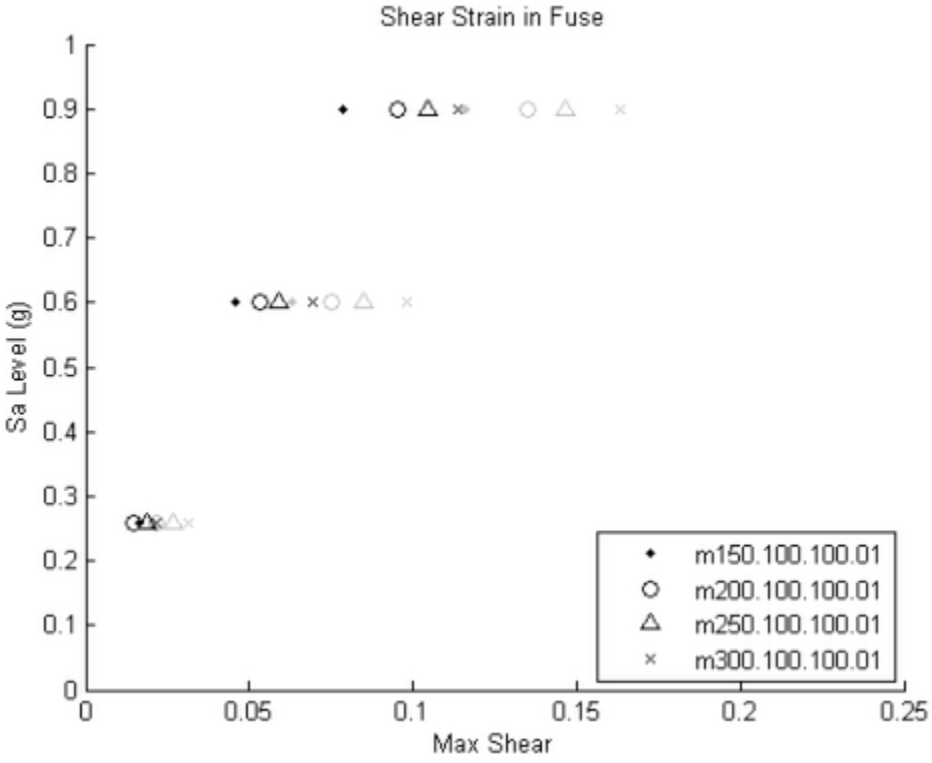

Figure 22 – A/B Study Peak Shear Strain Comparison

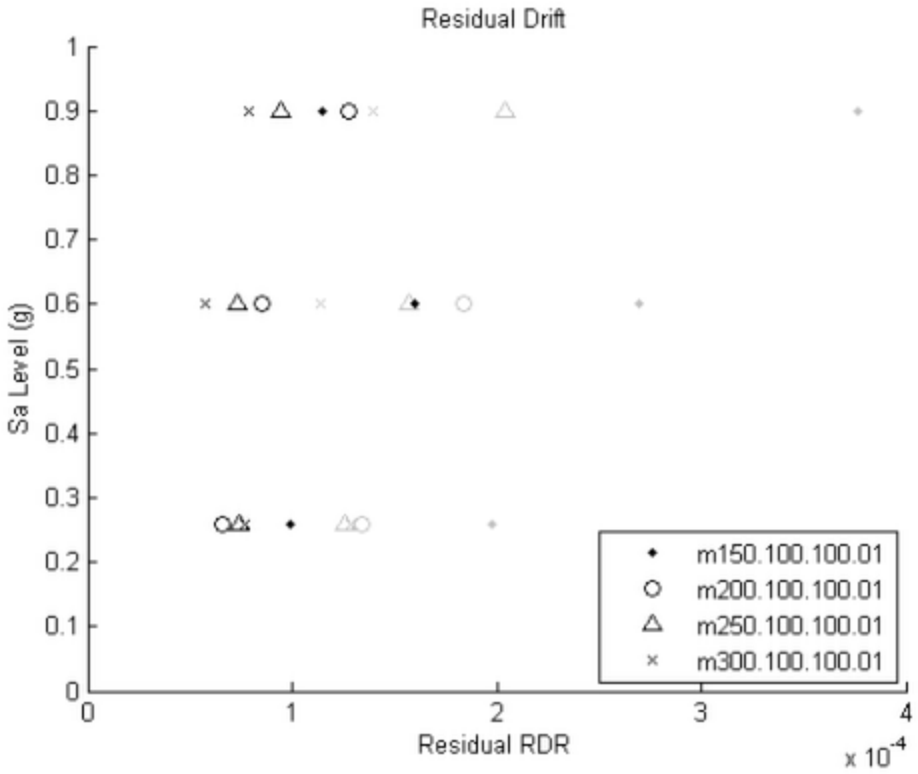

Figure 23 – A/B Study Residual Drift Comparison

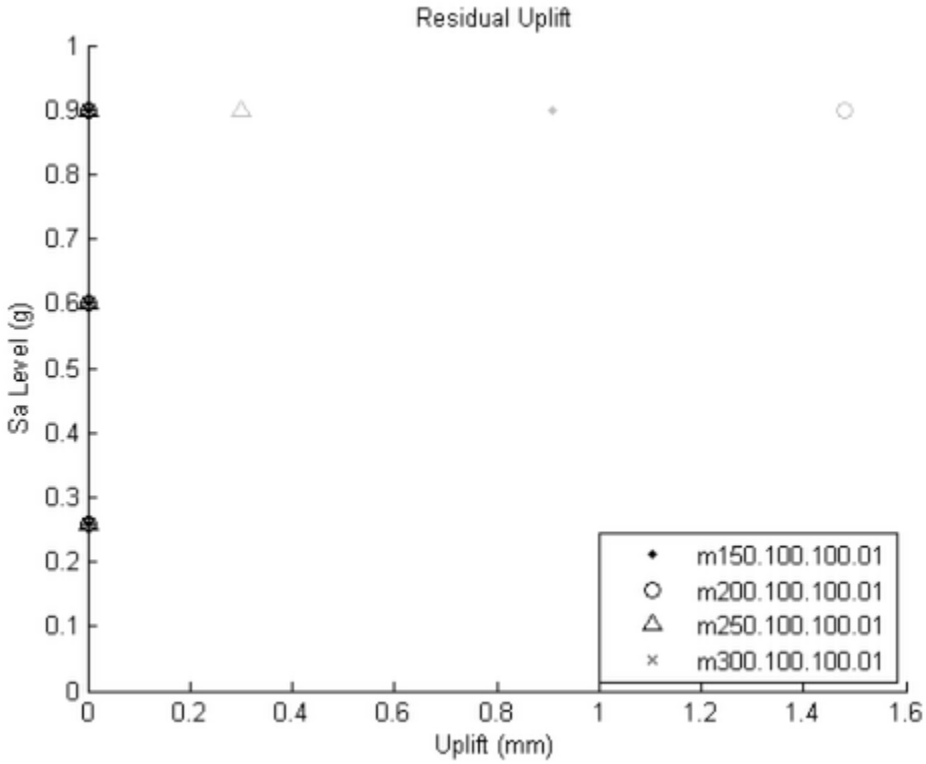

Figure 24 – A/B Study Residual Uplift Comparison

4.2 Overturning Factor

The overturning factor has a large effect on the energy dissipated at a given drift level, as well as the post-uplift stiffness. The larger PT area and fuse height required to raise the OT result in increased system stiffness and higher system yield strength. This greatly increases energy dissipation for a given drift (Figure 25). The roof drift ratio at the point of initial uplift also increases with OT, implying that a controlled rocking system designed for lower *R* will undergo more drift before uplifting. The higher stiffnesses associated with higher OT corresponded with lower natural periods (Figure 26). Increasing the OT reduces the peak displacements (Figure 27) and uplifts (Figure 28) significantly. By doubling the lateral strength of the system, the peak displacements and shear strains (Figure 33) are reduced by over 25%. The increased resistance to displacement corresponds with increases in peak base shear (Figure 29) and peak vertical base reaction (Figure 30) of 40% and 60% respectively. The peak accelerations are increased by 5-10%, likely due to the increased stiffness relative to the response spectra (Figure 31 and Figure 32). A small increase in the OT reduces residual displacements by an order of magnitude, to insignificant levels (Figure 34 and Figure 35).

It may be concluded that higher OT factors are favorable for minimizing displacement response, including residual displacements, and shear strains in the fuses. This must be tempered by the cost of larger forces that must be transmitted through the frame and foundation, and the fact that the system will lose appeal for higher OT values, which correspond to lower R factor values for this system.

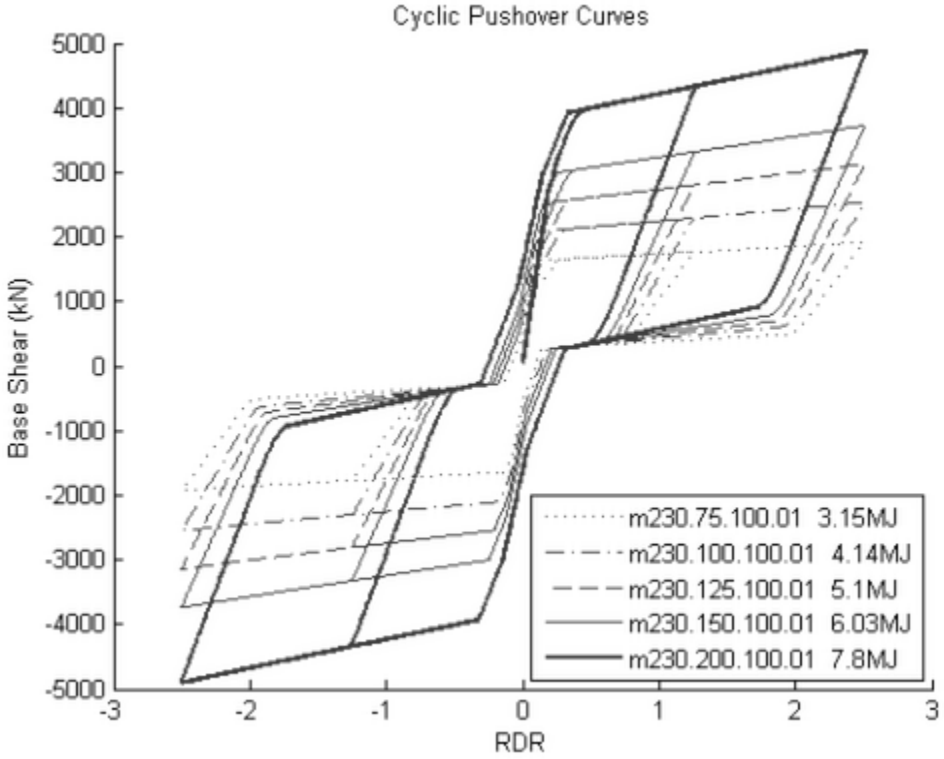

Figure 25 – OT Study Cyclic Pushover Comparison

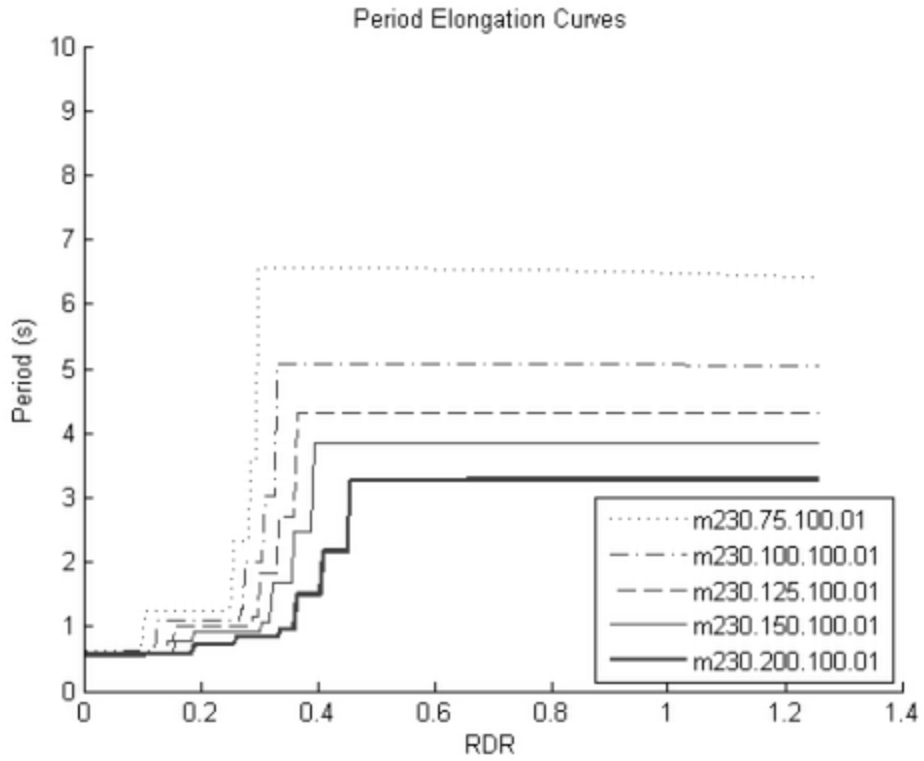

Figure 26 – OT Study Period During Pushover

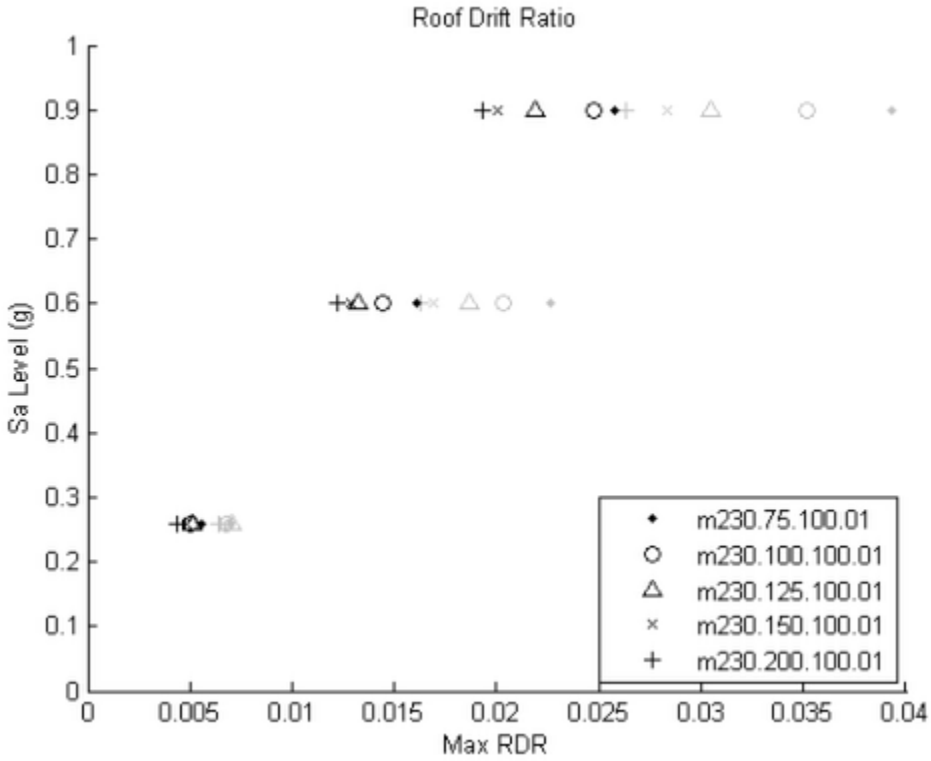

Figure 27 – OT Study Peak Roof Drift Ratio Comparison

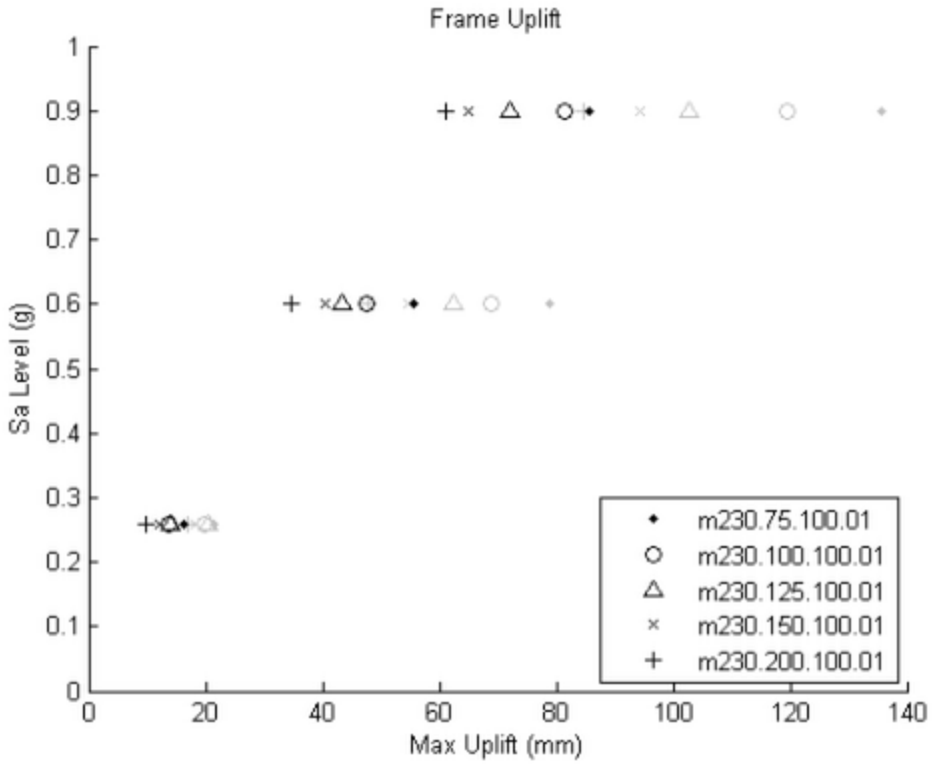

Figure 28 – OT Study Peak Uplift Comparison

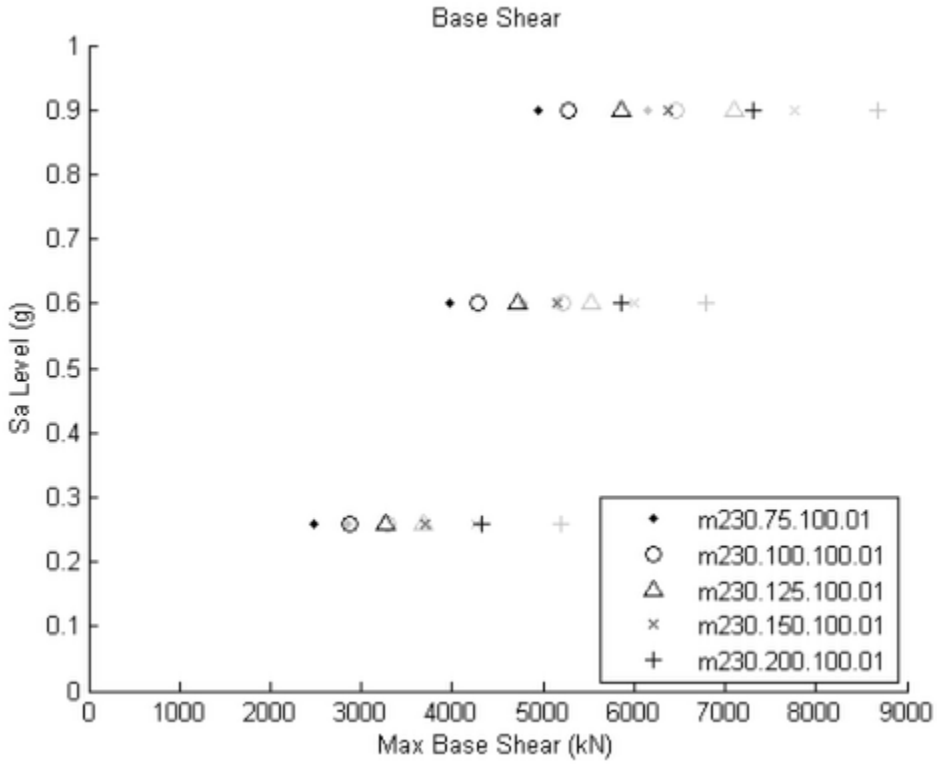

Figure 29 – OT Study Peak Base Shear Comparison

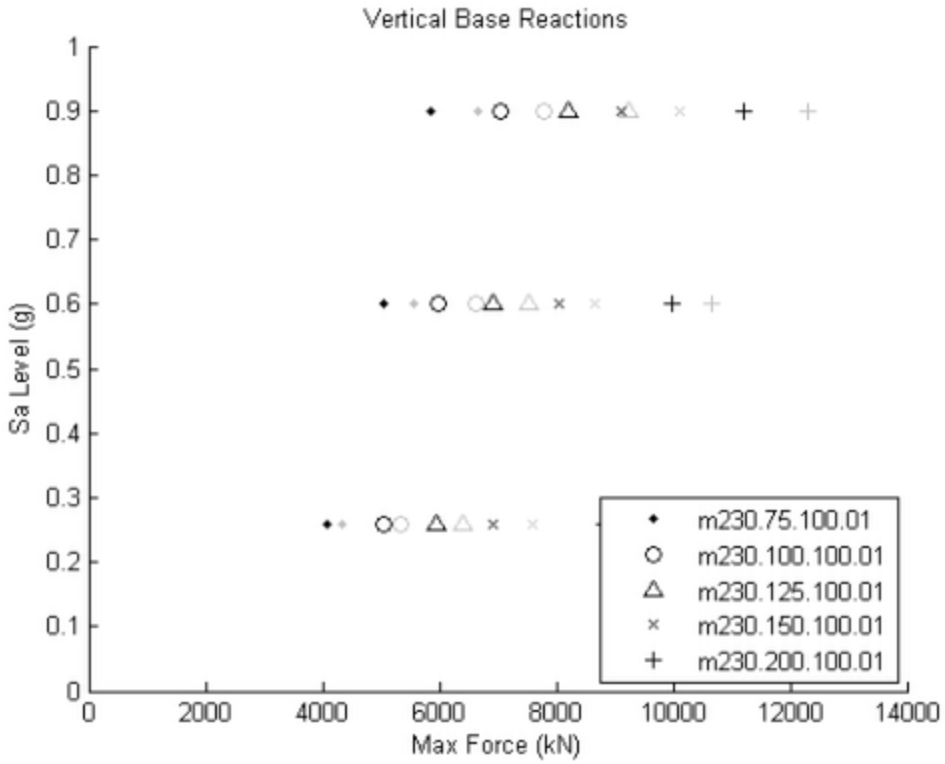

Figure 30 – OT Study Peak Vertical Base Reactions Comparison

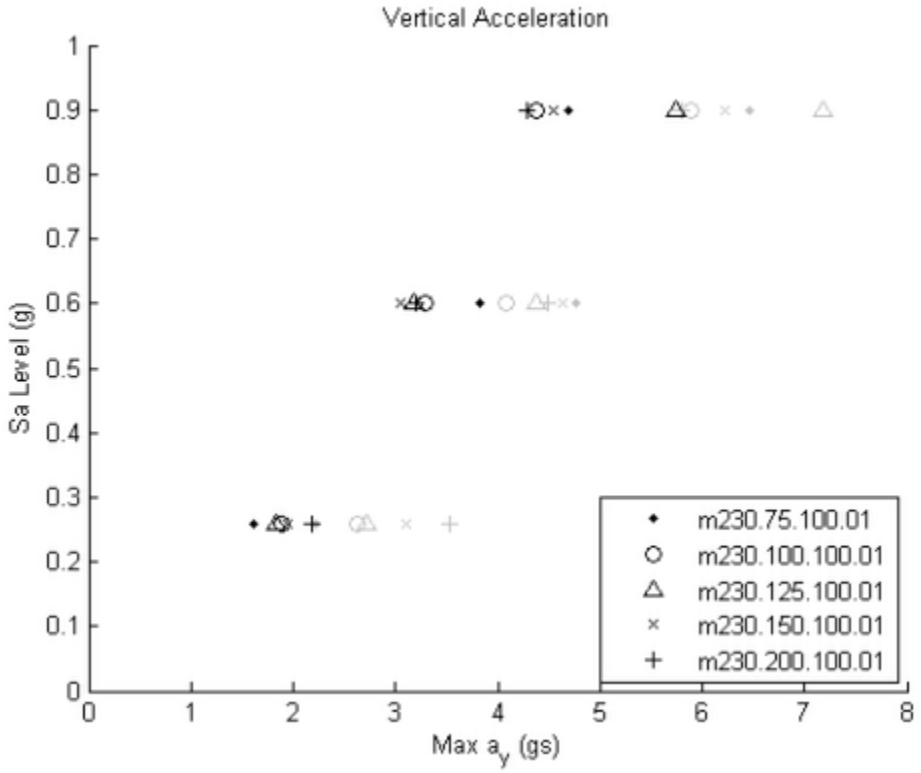

Figure 31 – OT Study Peak Vertical Acceleration Comparison

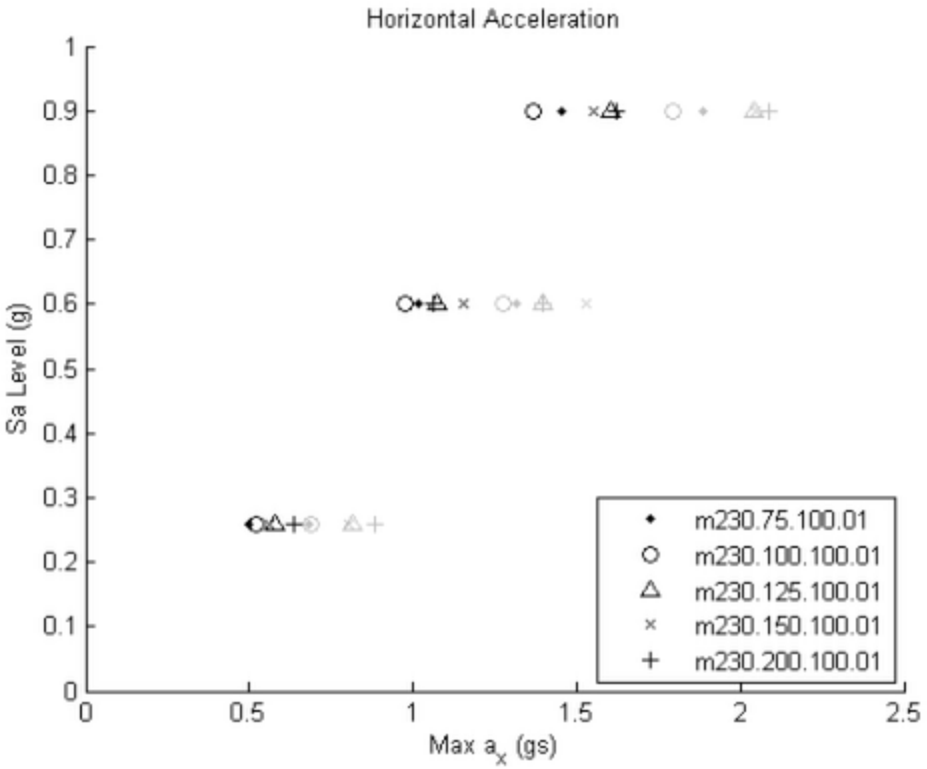

Figure 32 – OT Study Peak Horizontal Acceleration Comparison

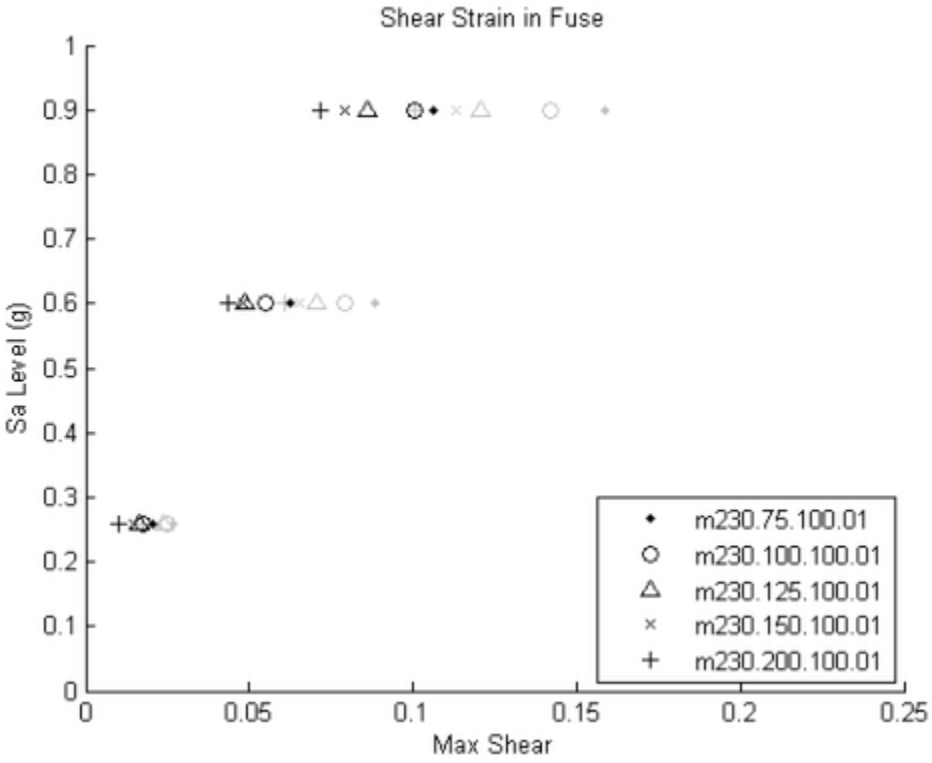

Figure 33 – OT Study Peak Shear Strain Comparison

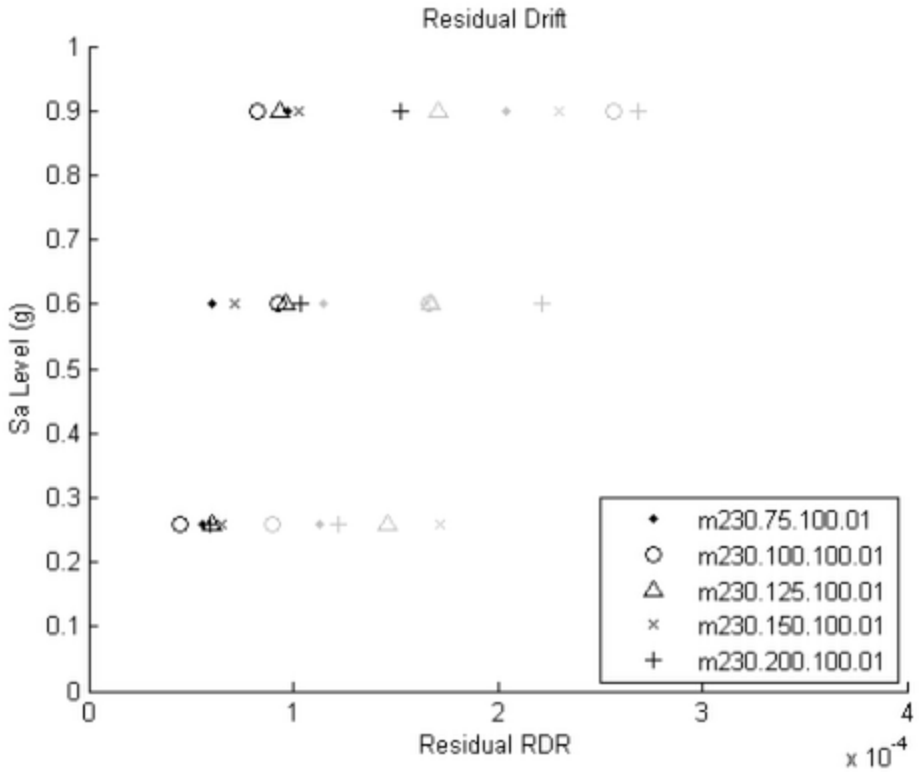

Figure 34 – OT Study Residual Drift Comparison

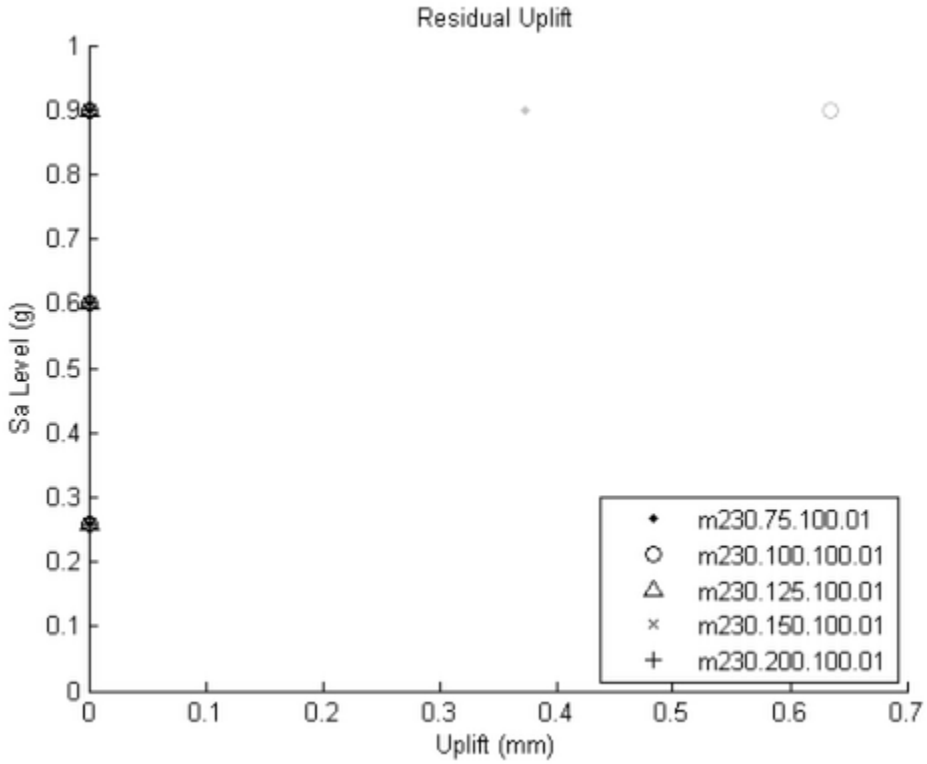

Figure 35 – OT Study Residual Uplift Comparison

4.3 Self-centering Factor

Variation of the self-centering factor has a major impact on the system response. The decrease in fuse strength relative to the PT strength associated with an increase in SC increases the base shear at which the system self-centers, sharply decreasing the energy dissipation (Figure 36). Increasing SC also delays uplift and increases the post-yield stiffness of the system. The higher SC factors exhibited lower periods (Figure 37). Since higher SC factors mean more PT and less fuse contribution, this implies that the PT contributes more to the system stiffness than the fuse and the fuse yield has a lesser effect on the system period. Increasing the self-centering factor has a minor negative effect on the time history displacements. Raising the SC from 1 to 2 increases the median peak roof drifts (Figure 38), uplift (Figure 39), and shear strains (Figure 44) by approximately 10%. It also increases the peak base shear (Figure 40) and vertical reactions by 10-15% (Figure 41) due to increased PT levels. The SC does not seem to have any correlation with accelerations (Figure 42 and Figure 43). Doubling the SC has a notable impact on the residuals (Figure 45 and Figure 46), although all of the residuals are still below the construction tolerances for new buildings.

The results show that it is not desirable to raise the SC. The system self-centers well at an SC of 1. It may even be desirable to lower SC slightly in some cases to decrease the response slightly.

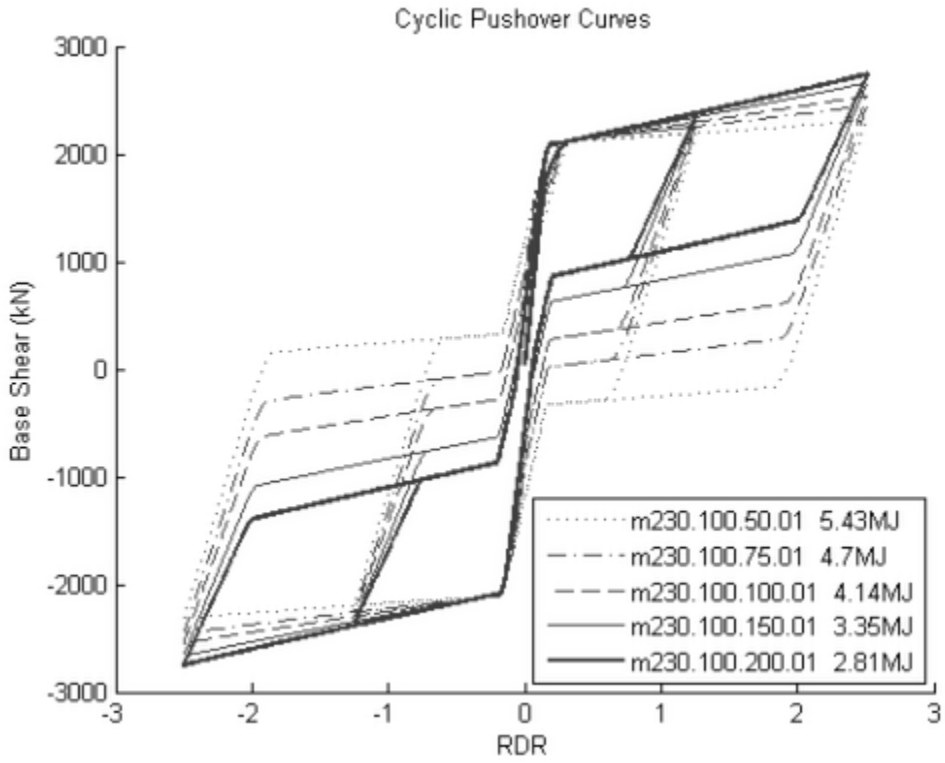

Figure 36 – SC Study Cyclic Pushover Comparison

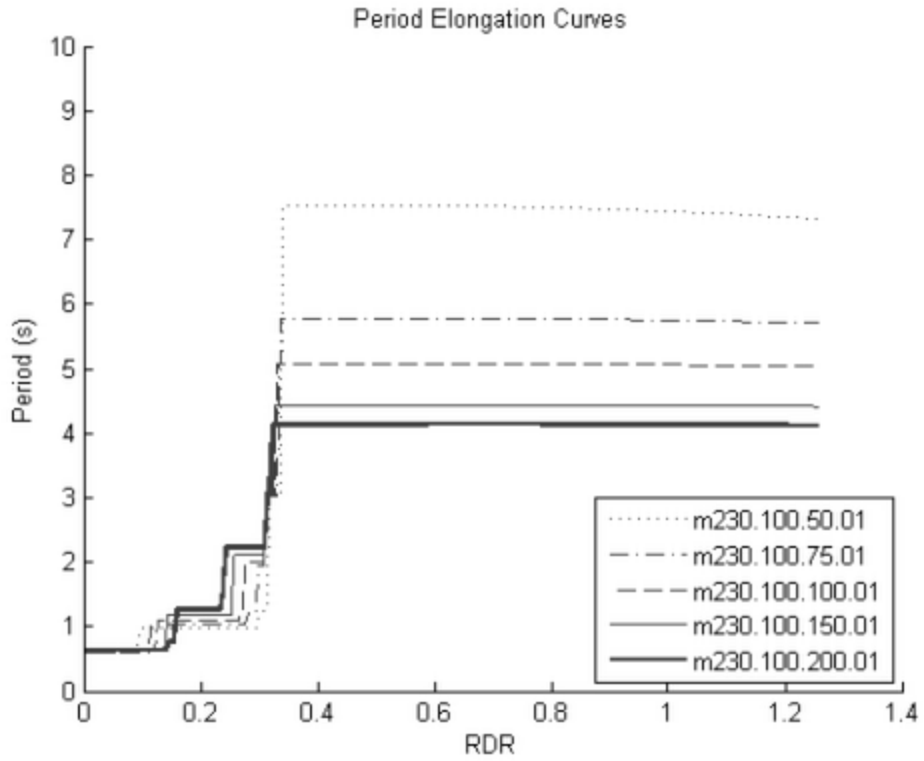

Figure 37 – SC Study Period During Pushover

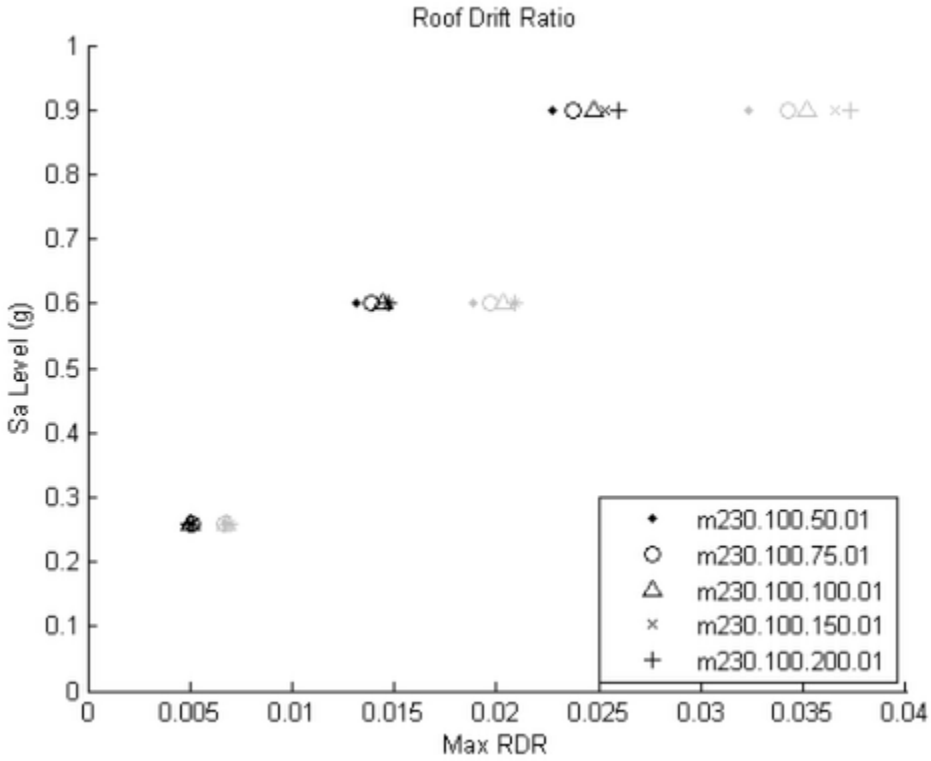

Figure 38 – SC Study Peak Roof Drift Ratio Comparison

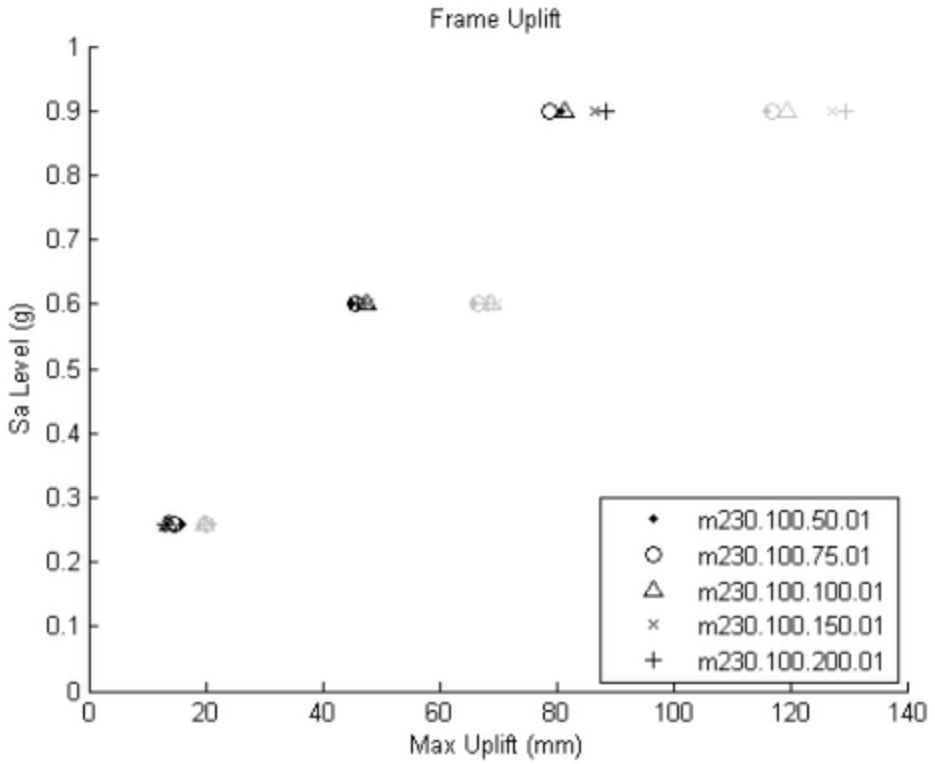

Figure 39 – SC Study Peak Uplift Comparison

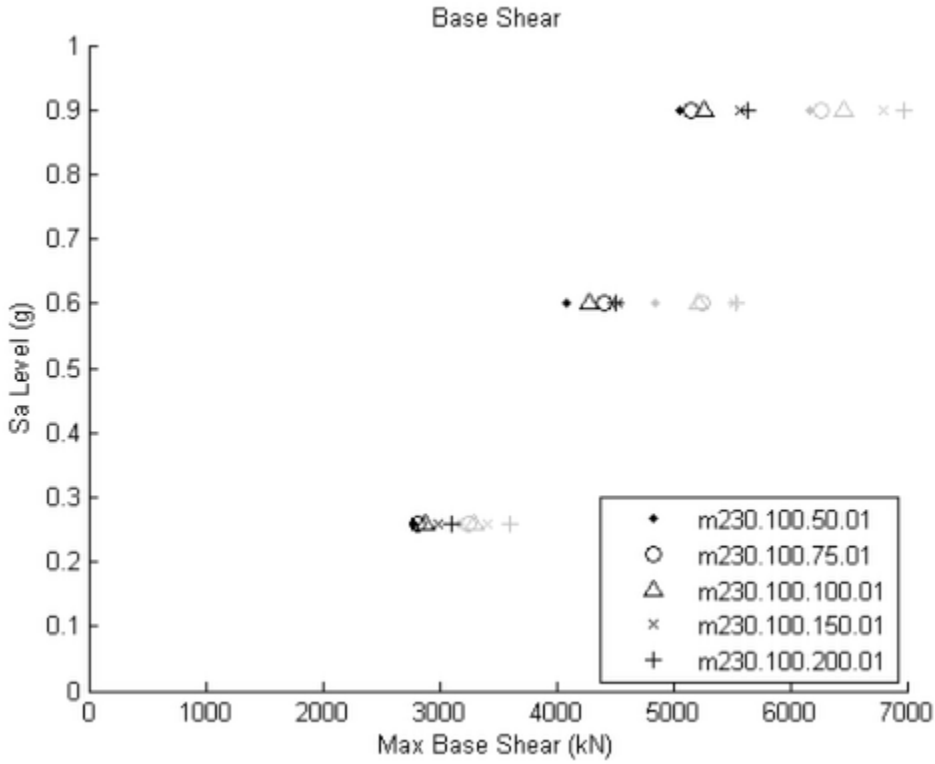

Figure 40 – SC Study Peak Base Shear Comparison

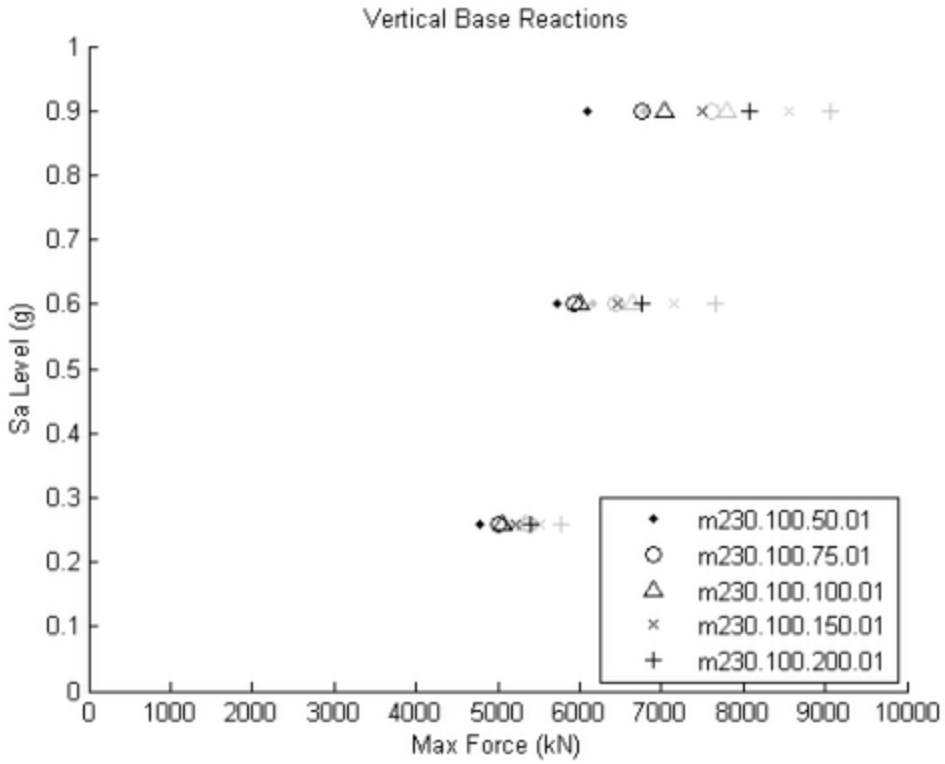

Figure 41 – SC Study Peak Vertical Base Reactions Comparison

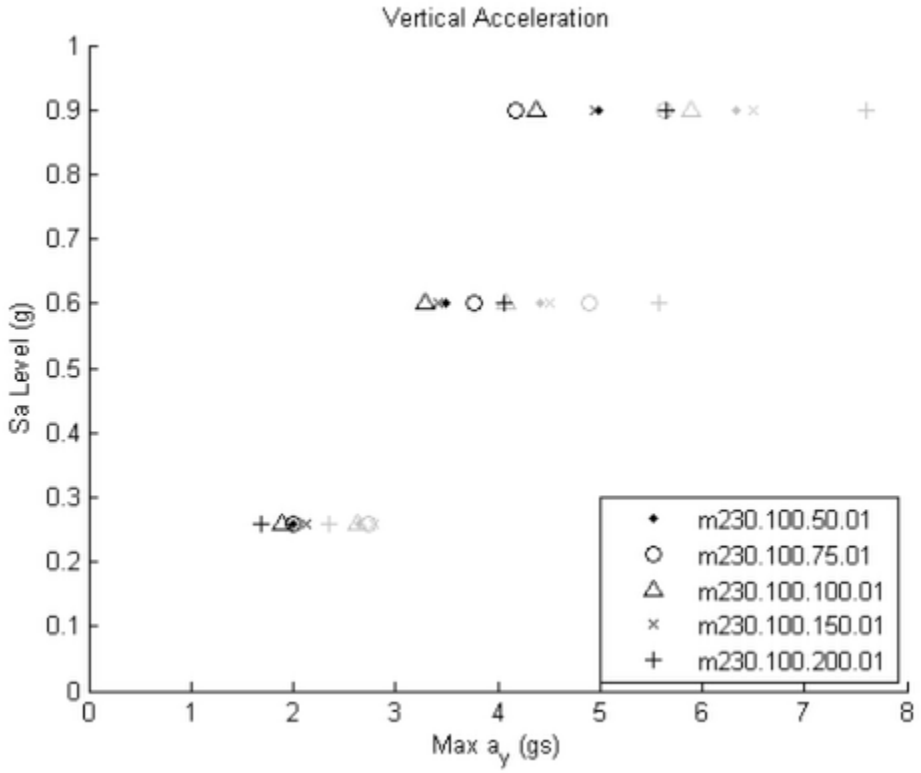

Figure 42 – SC Study Peak Vertical Acceleration Comparison

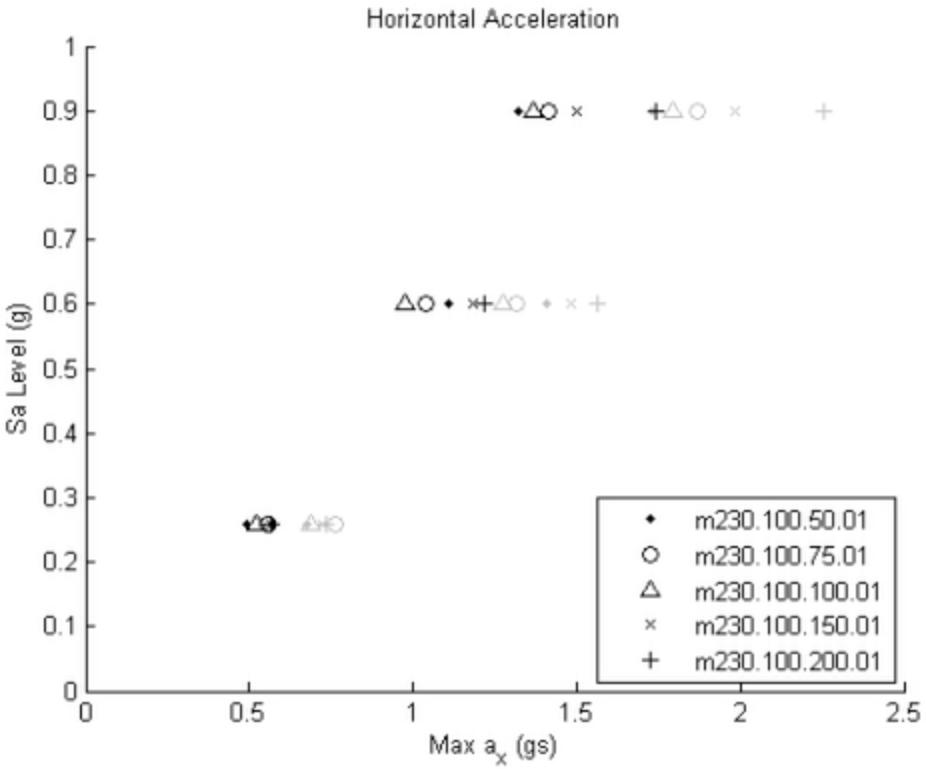

Figure 43 – SC Study Peak Horizontal Acceleration Comparison

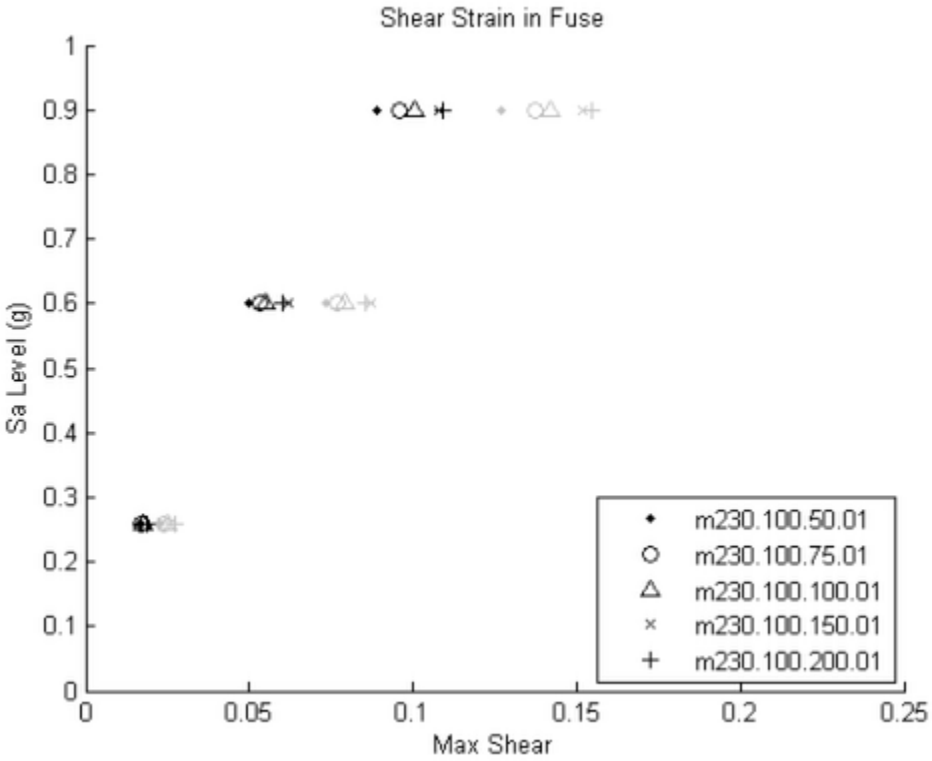

Figure 44 – SC Study Peak Shear Strain Comparison

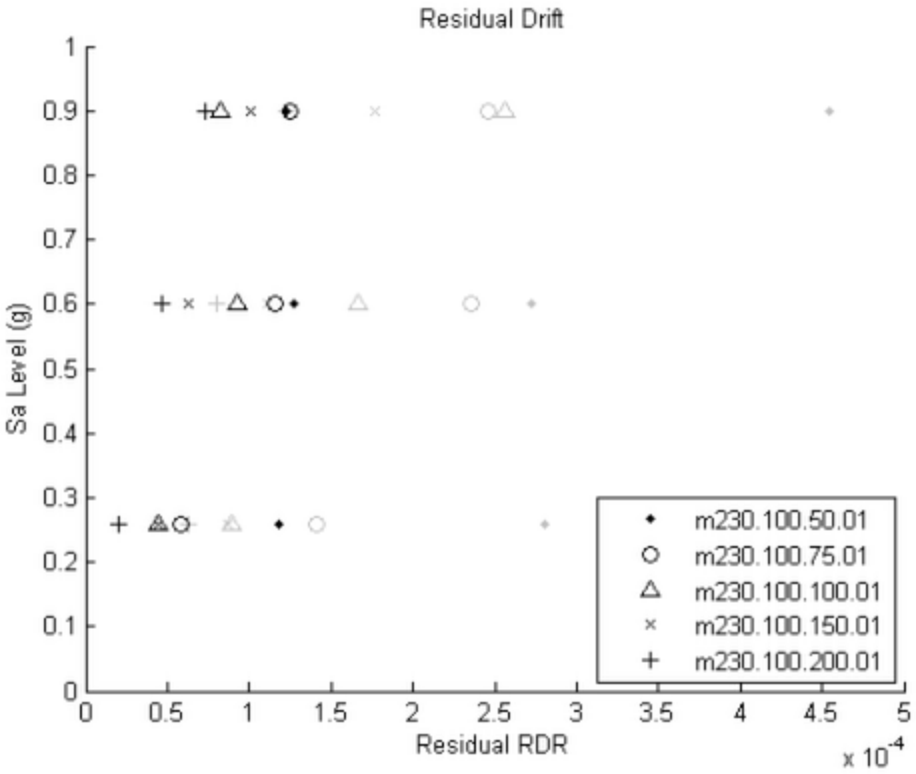

Figure 45 – SC Study Residual Drift Comparison

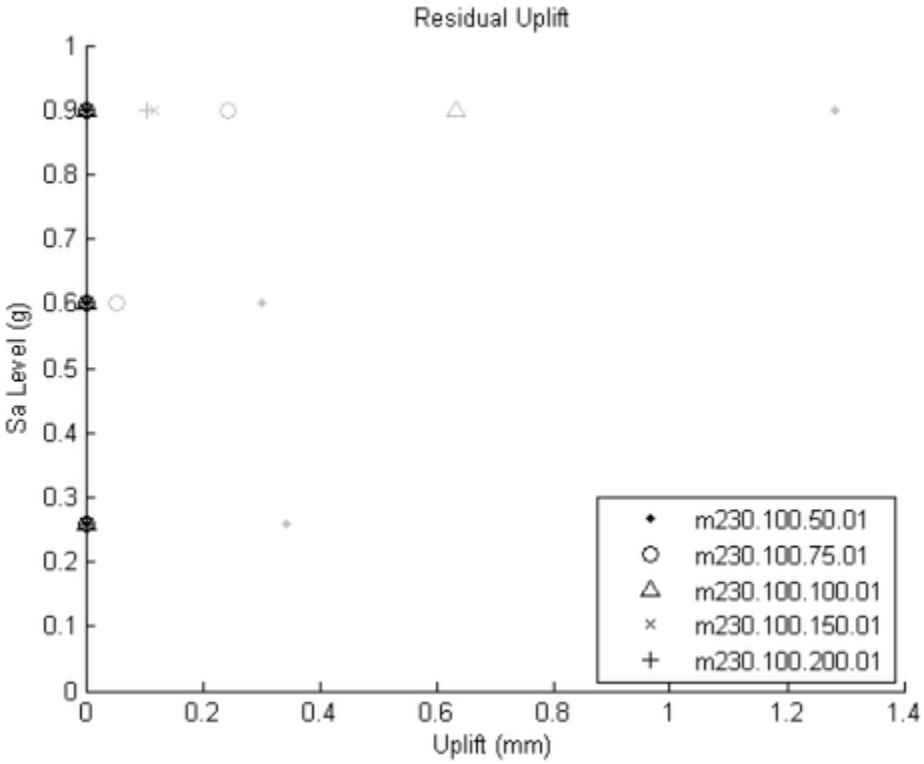

Figure 46 – SC Study Residual Uplift Comparison

4.4 Fuse Type

To explore the effects of different shear panel types on the system response, three fuse hysteretic types were compared, holding the A/B ratio constant at 2.3, the OT at 1.0, and the SC at 1.0. The three fuses considered were an elastic-perfectly plastic (EPP) slotted steel panel, an HPFRCC panel, and a deteriorating slotted steel panel. The constitutive relationship for fuse 1 was modeled after an EPP slotted steel panel with no pinching. This fuse was used in each of the previous studies for simplicity and because Hitaka provided equations for estimating the strength and stiffness. Fuse 3 uses a hysteresis obtained experimentally by a slotted steel panel test at Stanford. This research is ongoing and the strength degradation and pinching will likely be reduced following adjustments to the panel configuration. The constitutive relationship for fuse 2 is a fit to an experimental hysteresis from Canbolat et al. (2005) shown in Figure 4. For both fuses 2 and 3 the assumptions were made that the shape of the hysteresis would be unchanged by scaling the panel tests up to the prototype size and that the appropriate strength could be achieved by putting multiple panels in parallel. The key parameters used in the fuse constitutive relationships are shown in Table 3. Figure 47 shows the significance of these parameters in the pinching hysteresis. The hystereses of the three fuses are compared in Figure 48.

Table 3 – Fuse parameters

	Shear Yield Strain	Shear Yield Cap	Residual Strength Ratio	Post-Capping Slope Ratio	Pinching Force Factor	Pinching Displacement Factor
Fuse 1 – EPP	0.008	---	---	---	---	---
Fuse 2 – HPFRCC	0.01	0.03	0.75	-0.25	0.5	0.5
Fuse 3 – Steel	0.01	0.036	0.10	-0.036	0.7	0.5

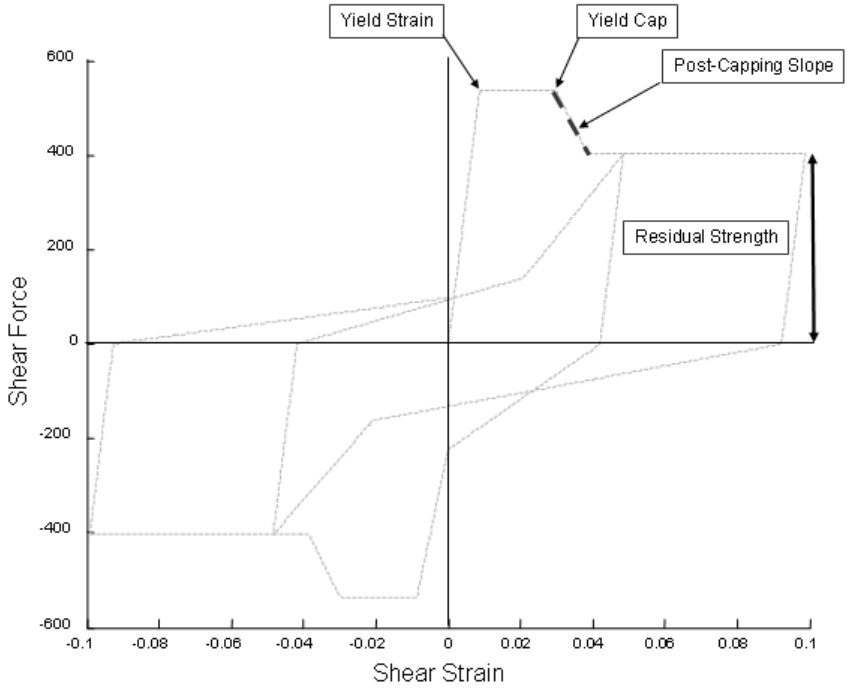

Figure 47 – Pinching Hystereses Diagram

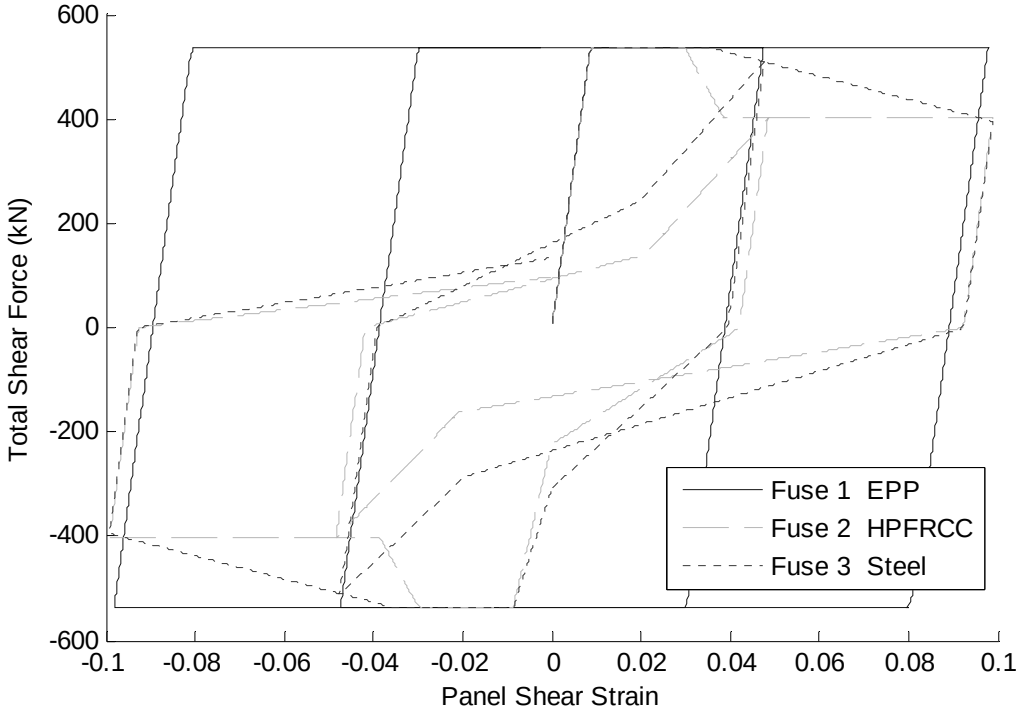

Figure 48 – Fuse Hystereses Comparison

The strength degradation and pinching of fuses 2 and 3 had a significant effect on the response of the system. The pushover shows a 40% reduction of energy dissipation from the EPP fuse (Figure 49). The peak displacement responses of the pinching fuses (Figure 38, Figure 39, and Figure 44) were increased by approximately 20%. Fuse 3, which had less degradation and pinching than fuse 2, had slightly smaller peak displacements. Differences in peak base reactions and accelerations (Figure 53, Figure 54, Figure 55, and Figure 56). As suggested by the cyclic pushover curves, the median residual displacements are lower for the pinching fuses (Figure 58 and Figure 59), however the standard deviations of the residuals are larger for pinching fuses. Further investigation showed that the standard deviations were skewed by high residual displacements from one ground motion record, LP89svl. If the statistics are recalculated excluding this record, the standard deviations also indicate lower residuals for pinching fuses (Figure 60 and Figure 61).

These results confirm that fuses with strength degradation and pinching have a negative effect on the peak displacements. Pinching fuse hystereses do improve the self-centering ability of the system, but the residual drifts with non-pinching fuses were small enough that repair would be unnecessary. Generally, fuses higher energy dissipation will be more desirable.

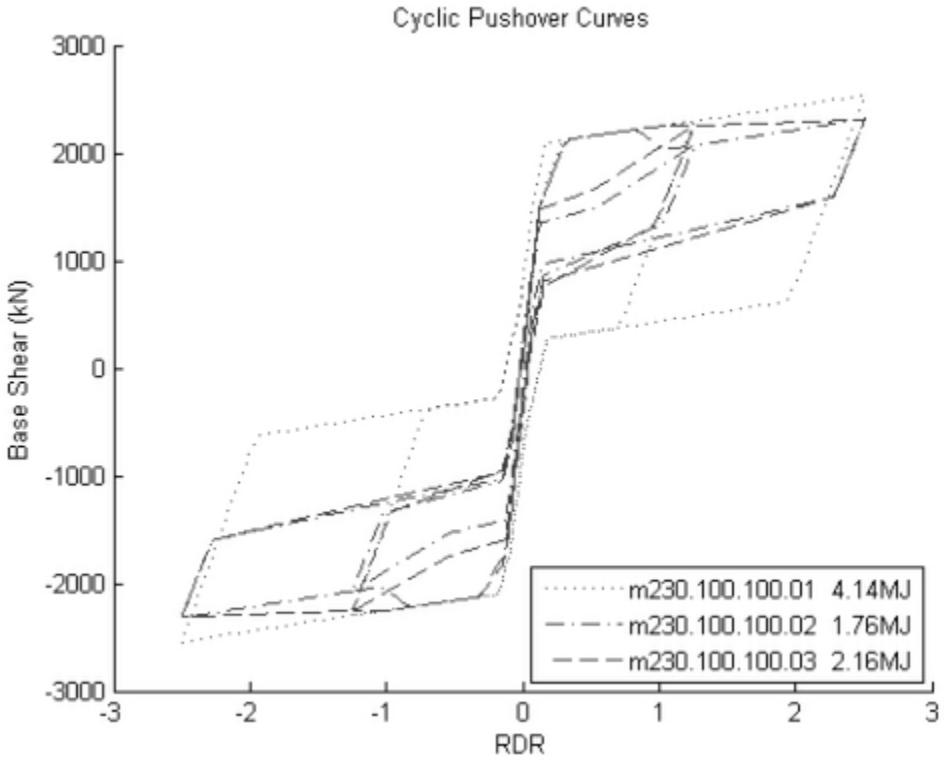

Figure 49 – Fuse Study Cyclic Pushover Comparison

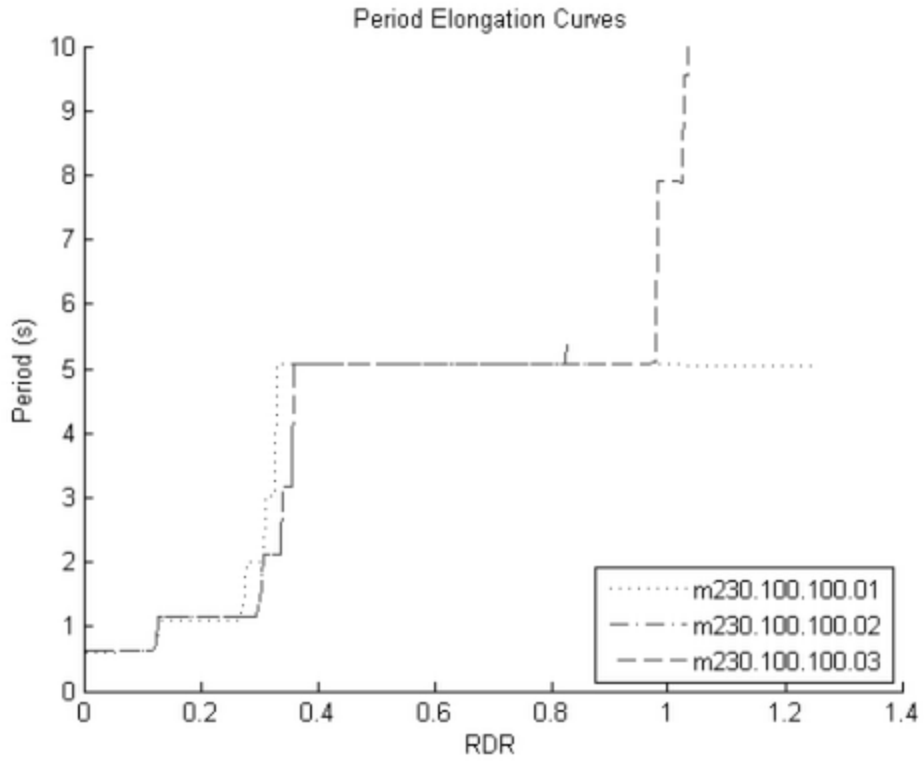

Figure 50 – Fuse Study Period During Pushover

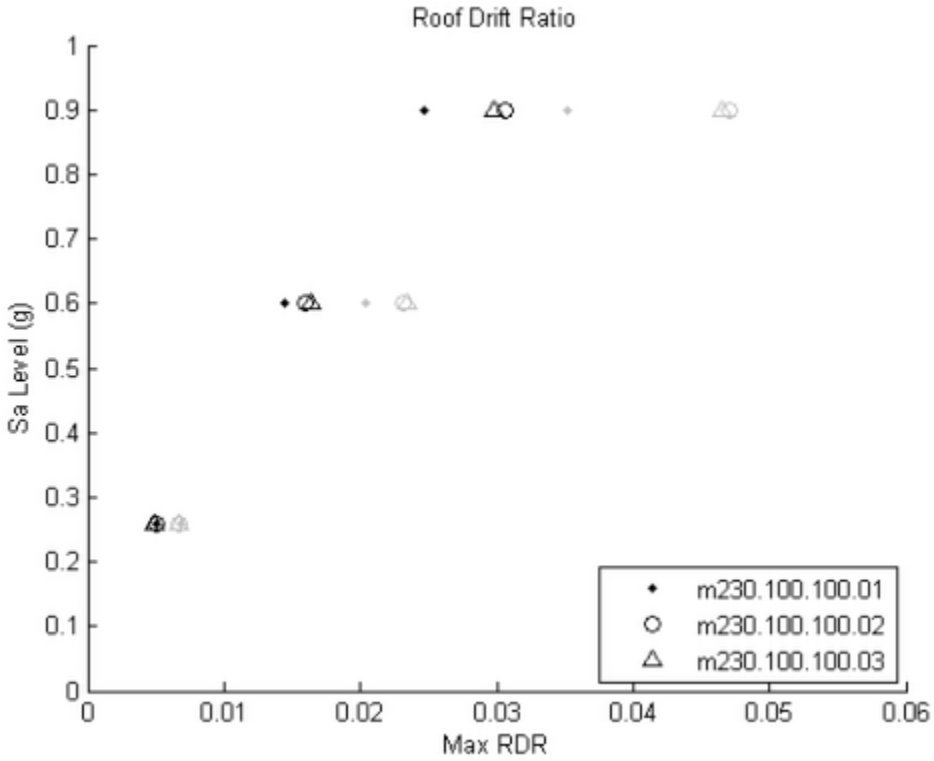

Figure 51 – Fuse Study Peak Roof Drift Ratio Comparison

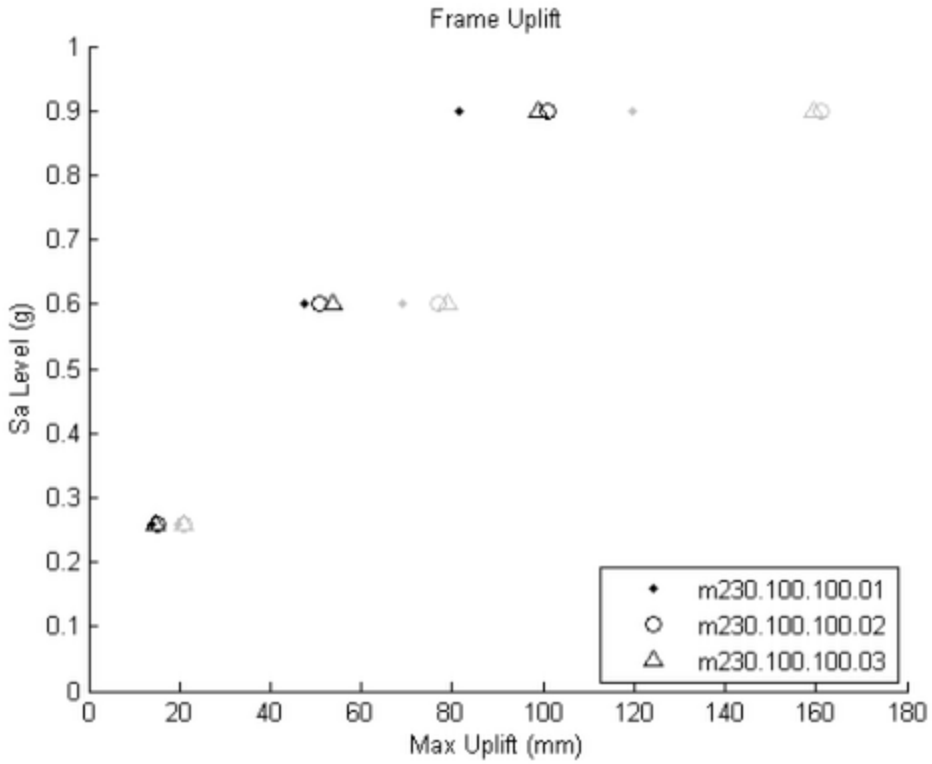

Figure 52 – Fuse Study Peak Uplift Comparison

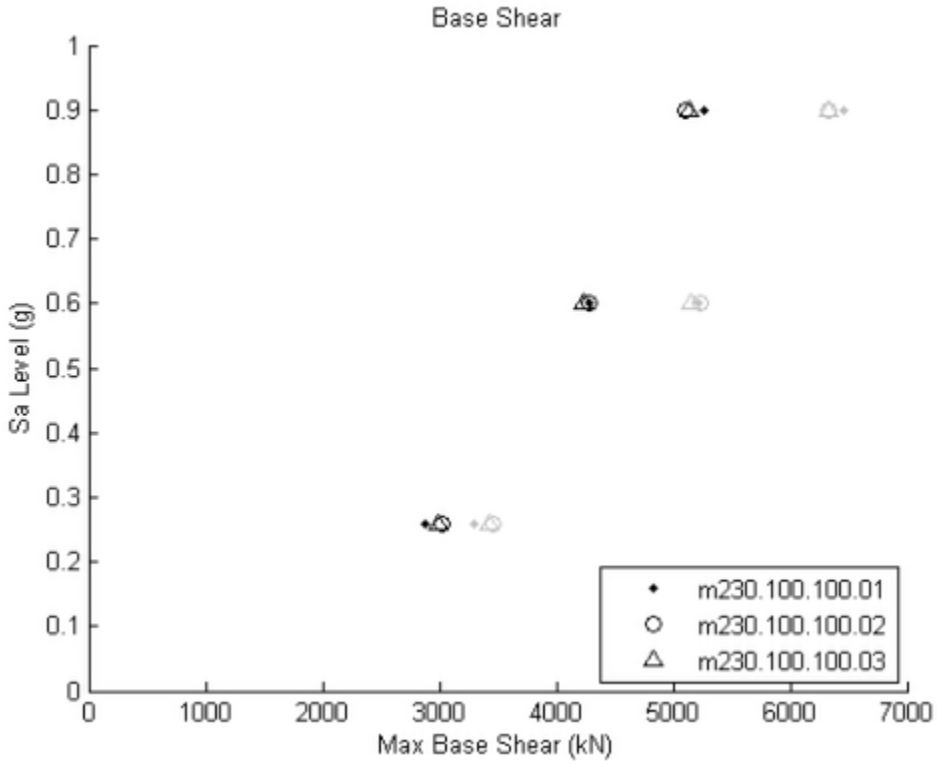

Figure 53 – Fuse Study Peak Base Shear Comparison

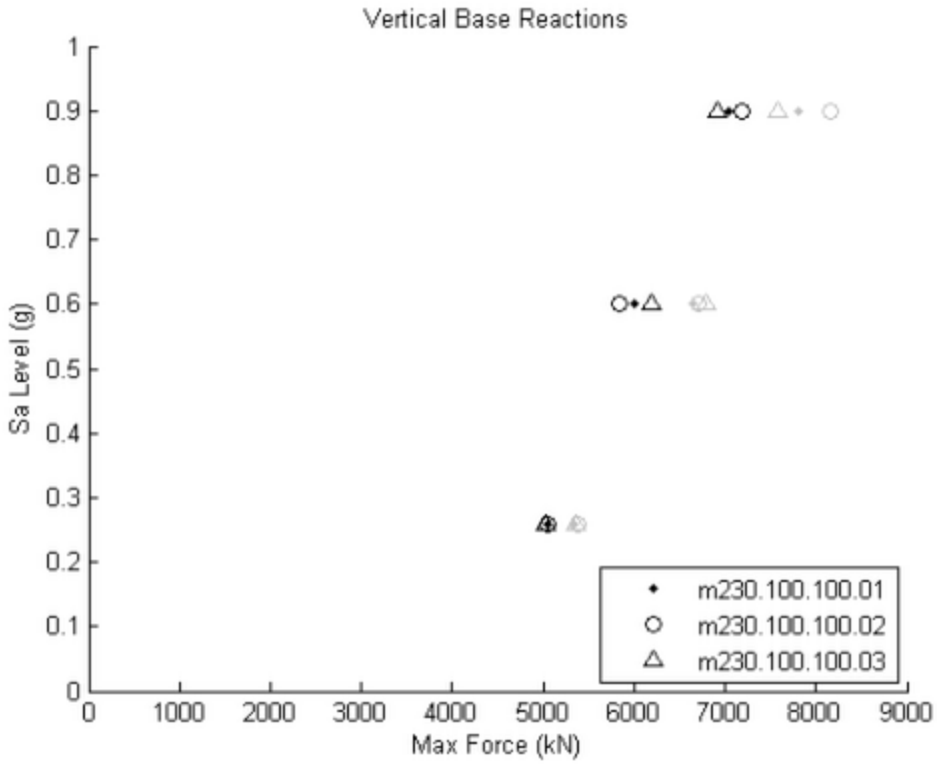

Figure 54 – Fuse Study Peak Vertical Reaction Comparison

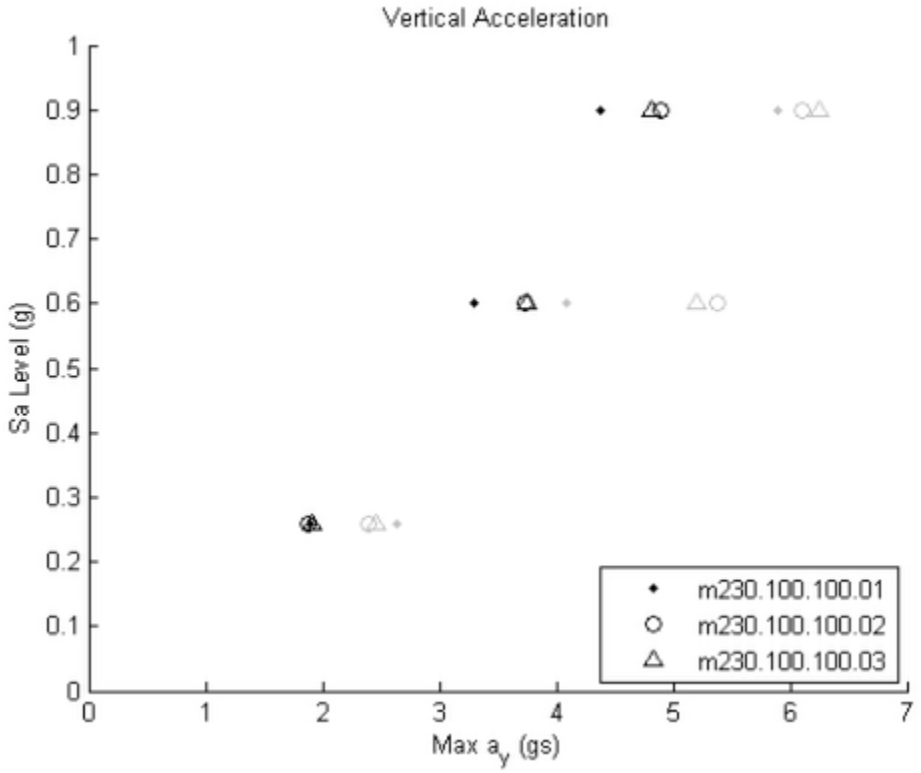

Figure 55 – Fuse Study Peak Vertical Acceleration Comparison

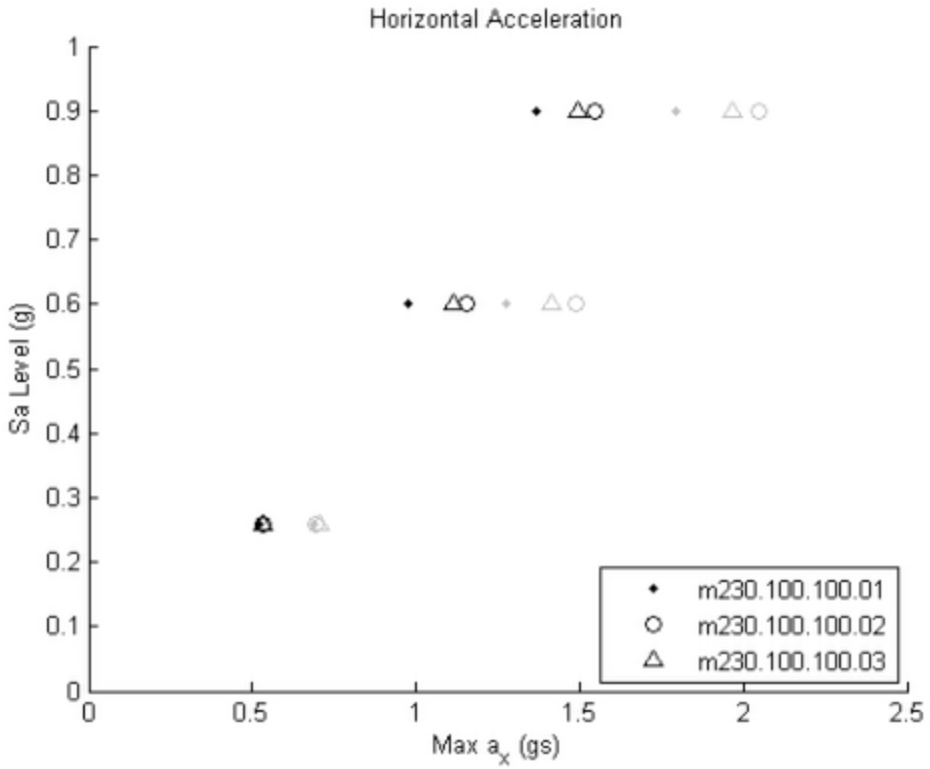

Figure 56 – Fuse Study Peak Horizontal Acceleration Comparison

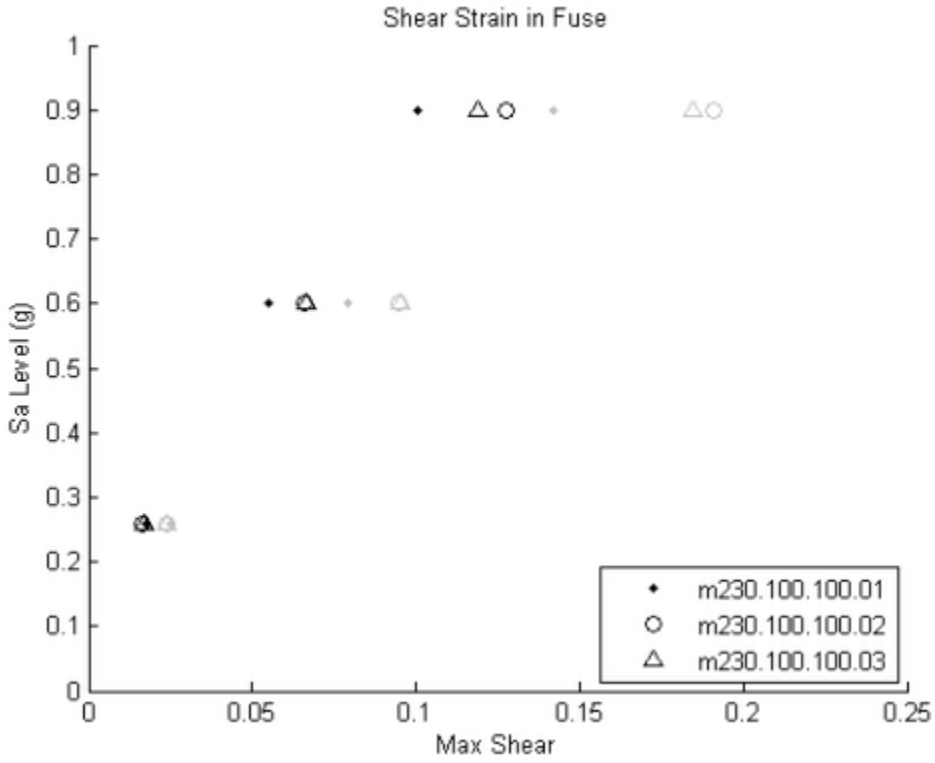

Figure 57 – Fuse Study Peak Shear Strain Comparison

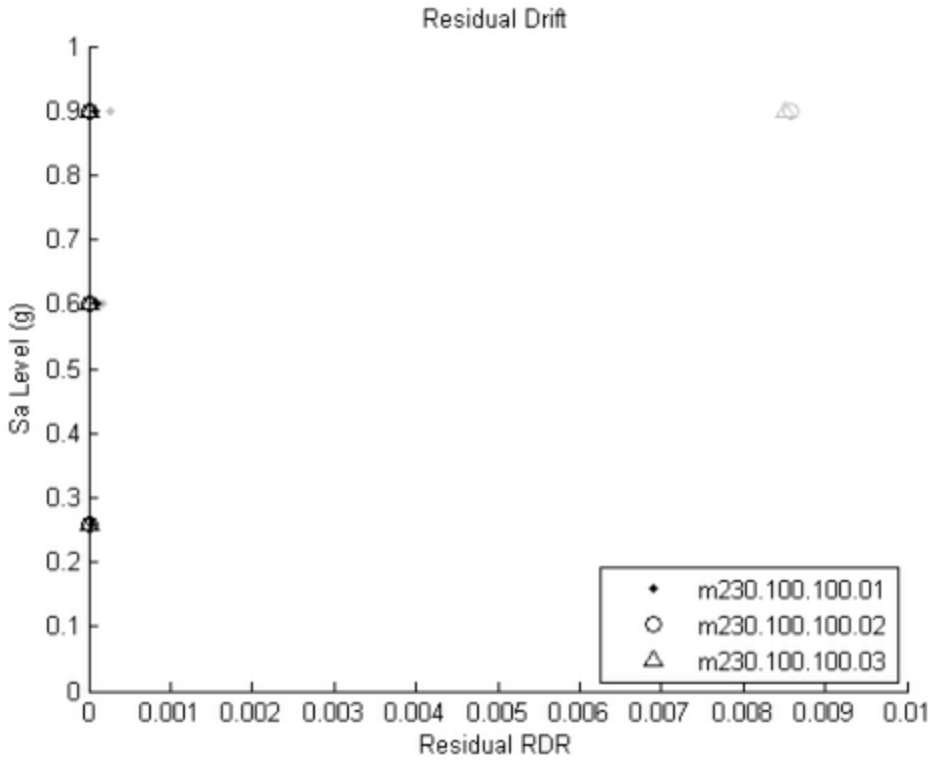

Figure 58 – Fuse Study Residual Drift Comparison

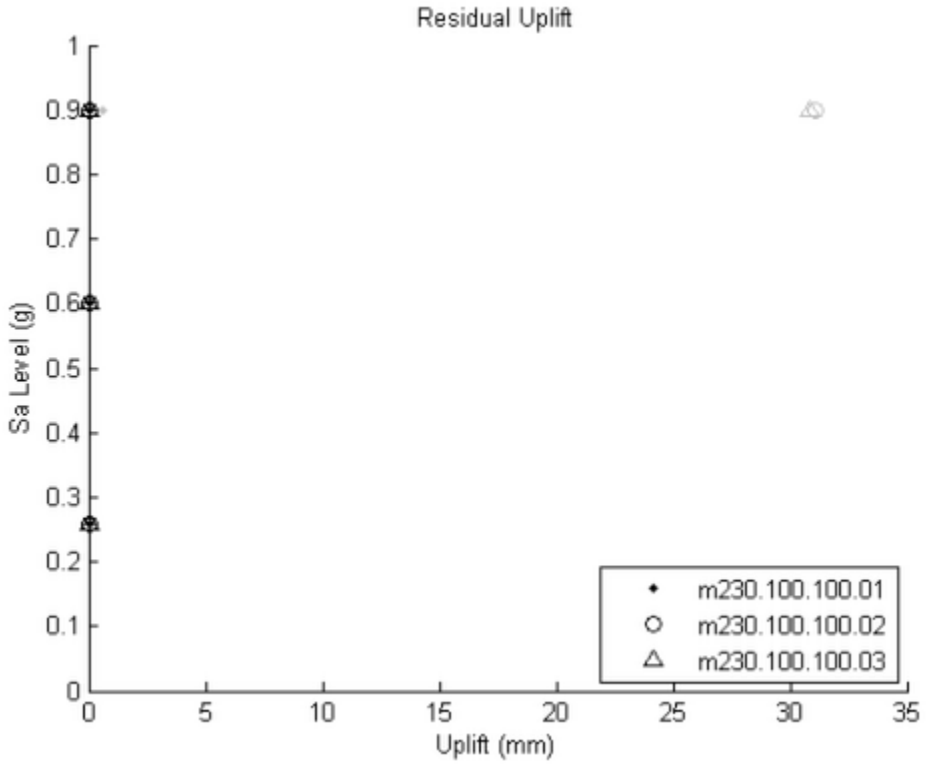

Figure 59 – Fuse Study Residual Uplift Comparison

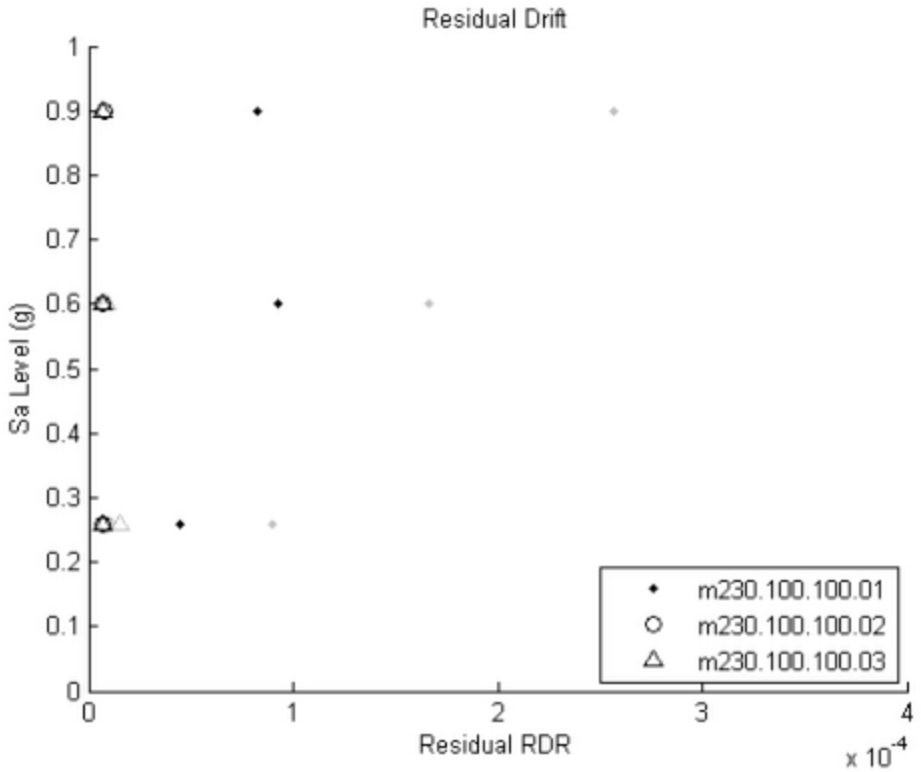

Figure 60 – Fuse Study Residual Drifts Excluding LP89svl

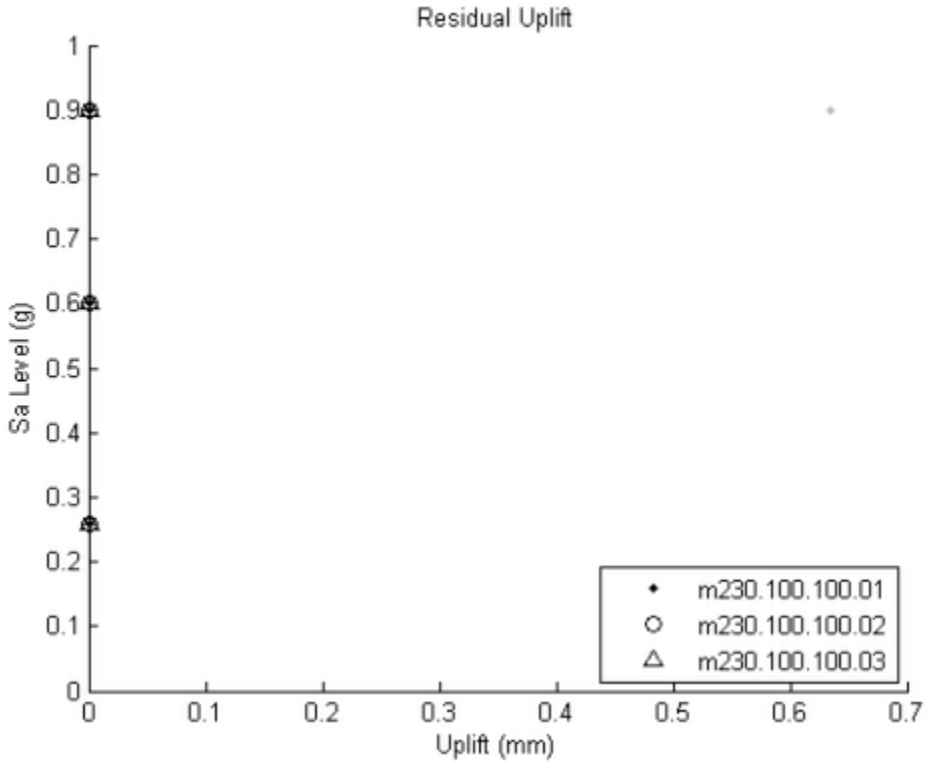

Figure 61 – Fuse Study Residual Uplifts Excluding LP89svl

CONCLUSION

These results show that the reduction of the A/B ratio primarily resulted in a decrease in the fuse shear strains, keeping in mind that this will result in steeper bracing in the braced frames, and slightly higher displacements. Higher OT factors are favorable for minimizing displacement response, including residual displacements, and to some extent the shear strains in the fuses (which may also be controlled by varying A/B). The advantages of increasing OT must be tempered by the cost of larger forces that must be transmitted through the frame and foundation, and slightly larger accelerations. In addition, the system will lose appeal for higher OT values, which correspond to lower R factor values for this system (OT = 1 corresponds to R = 8; OT = 2 corresponds to R = 4). The SC value might be best left at 1.0 or slightly lower. Lowering it too much would put the structure at risk for global overturning, i.e., the full uplift of one frame due to the fuse overcoming gravity and the PT. This global overturning limit on SC varies with the A/B ratio. The fuses are an ongoing area of research. Analysis results confirm that the development of shear panels with the highest energy dissipation will significantly improve system performance. The fuse is a central and essential component.

Thus, the most likely design scenario is OT = 1.0, SC = 1.0, and then practitioners must vary their A/B ratio to match their plan conditions. Recommendations will likely be needed that then tie the maximum permissible A/B ratio to the fuse shear strain capacity. The larger the fuse shear strain capacity, the larger the permissible A/B ratio. This study shows that, based on 2% in 50 year results, for a fuse shear strain capacity of 0.08, the maximum A/B ratio should be set at 1.5 – that is very restrictive. For a fuse shear strain capacity of 0.10, the maximum A/B ratio should be 2.0. For a fuse shear strain capacity of 0.11, the maximum A/B ratio should be 2.5. For a fuse shear strain capacity of 0.13, the maximum A/B ratio should be 3.0. Thus, the fuse strain shear capacity is crucial for the flexibility of this system. These values are approximate and dependent on the ground motions chosen, and the fact that this is a three-story prototype structure with a specific amount of gravity load on it.

The alternative is to somehow add more strength (increase OT) to the frame (e.g., through energy dissipating devices at the column bases that delay initial uplift) without considering the R factor to be decreased (if such is possible). Increasing OT will lower the displacements (peak and residual) and fuse strains. That is, at R = 8, clearly this system must rock and strain the fuses to achieve this high level of ductility.

At this time, it is thus necessary to evaluate whether there are any concerns with frame designs having OT = 1, SC = 1 and any A/B between 1.5 and 3, other than the fuse shear strains. In addition, are there concerns about the sensitivity of this system if engineers have OT and SC values that vary from 1.0 for whatever reasons (note the rest of the building structure may raise or lower these values). Generally raising OT has positive benefits, and lowering OT is unlikely as the provisions will be strength based. Raising SC may limit energy dissipation. Lowering SC does not seem to have severe negative ramifications so long as the small cyclic cycles at the end of the earthquake help to ensure self-centering.

References

Ajrab, J. J., Pekcan, G., and Mander, J. B. (2004). "Rocking Wall-Frame Structures with Supplemental Tendon Systems," *Journal of Structural Engineering*, ASCE, Vol. 130, No. 6, June 1, 2004.

Azuhata, T., Midorikawa, M., and Wada, A. (2003). "Study on Applicability of Rocking Structural Systems to Building Structures," *Smart Structures and Materials 2003: Damping and Isolation*, Proceedings of SPIE Vol. 5052.

Canbolat, B. A., Parra-Montesinos, G. J., and Wight, J. K. (2005). "Experimental Study on Seismic Behavior of High-Performance Fiber-Reinforced Cement Composite Coupling Beams," *ACI Structural Journal*, January-February.

Chen, Y.-H., Liao, W.-H., Lee, C.-L., and Wang, Y.-P. (2006). "Seismic Isolation of Viaduct Piers by Means of a Rocking Mechanism," *Earthquake Engineering and Structural Dynamics*, February 10, 2006, Vol. 35 pp 713-736.

Christopoulos, C., Filiatrault, A., and Folz, B. (2002). "Seismic Response of Self-Centering Hysteretic SDOF Systems," *Earthquake Engineering and Structural Dynamics*, Vol. 31 pp 1131-1150.

Hitaka, Toko and Matsui, Chiaki (2003). "Experimental Study on Steel Shear Wall with Slits," *Journal of Structural Engineering*, ASCE, Vol. 129, No. 5, May.

Li, V. C., Mishra, D. K., Naaman, A. E., Wight, J. K., LaFave, J., M., Wu, H.-C., and Inadab, Y. (1994). "On the Shear Behavior of Engineered Cementitious Composites," *Advanced Cement Based Materials*, Vol. 1, No. 3 , March, pp. 142-149.

Makris, Nicos and Konstantinidis (2002). "The Rocking Spectrum and the Limitations of Practical Design Methodologies," Earthquake Engineering and Structural Dynamics, Vol. 32, pp 265-289.

Meek, J. W. (1975). "Effects of Foundation Tipping on Dynamic Response," *Journal of the Structural Division*, ASCE, Vol. 101, No. 7, pp. 1297-1311.

Pacific Earthquake Engineering Research Center (2000). Strong Motion Database, August 25, 2006, < http://peer.berkeley.edu/smcat/index.html>.

Pekcan, G., Mander J. B., and Chen, S. S. (2000). "Experiments on Steel MRF Building With Supplemental Tendon System," ASCE Journal of Structural Engineering Vol. 126, No. 4 April 2000.

Sause, R., Ricles, J. M., Roke, D., and Seo, C.-Y. (2006). “Self-Centering Seismic-Resistant Steel Concentrically Braced Frames,” Proceedings of the Fifth International Conference on Behaviour of Steel Structures in Seismic Areas, STESSA 2006, August 14-17, Yokohama, Japan.

Toranzo, L.A., Carr, A.J., Restrepo, J.I. (2001). “Displacement Based Design of Rocking Walls Incorporating Hysteretic Energy Dissipators,” 7th International Seminar on Seismic Isolation, Passive Energy Dissipation and Active Control of Vibrations of Structures, Assisi, Italy, October 2-5, 2001.

Wolski, M., Ricles, J.M., Sause, R. (2006). “Seismic Resistant Self-Centering Steel Moment Resisting Frames With Bottom Flange Friction Devices,” Proceedings of the Fifth International Conference on Behaviour of Steel Structures in Seismic Areas, STESSA 2006, August 14-17, 2006, Yokohama, Japan.

List of Recent NSEL Reports

No.	*Authors*	*Title*	*Date*
011	Gao, Y. and Spencer, B.F.	Structural Health Monitoring Strategies for Smart Sensor Networks	May 2008
012	Andrews, B., Fahnestock, L.A. and Song, J.	Performance-based Engineering Framework and Ductility Capacity Models for Buckling-Restrained Braces	July 2008
013	Pallarés, L. and Hajjar, J.F.	Headed Steel Stud Anchors in Composite Structures: Part I – Shear	April 2009
014	Pallarés, L. and Hajjar, J.F.	Headed Steel Stud Anchors in Composite Structures: Part II – Tension and Interaction	April 2009
015	Walsh, S. and Hajjar, J.F.	Data Processing of Laser Scans Towards Applications in Structural Engineering	June 2009
016	Reneckis, D. and LaFave, J.M.	Seismic Performance of Anchored Brick Veneer	Aug. 2009
017	Borello, D.J., Denavit, M.D., and Hajjar, J.F.	Behavior of Bolted Steel Slip-critical Connections with Fillers	Aug. 2009
018	Rice, J.A. and Spencer, B.F.	Flexible Smart Sensor Framework for Autonomous Full-scale Structural Health Monitoring	Aug. 2009
019	Sim, S.-H. and Spencer, B.F.	Decentralized Strategies for Monitoring Structures using Wireless Smart Sensor Networks	Nov. 2009
020	Kim, J. and LaFave, J.M.	Joint Shear Behavior of Reinforced Concrete Beam-Column Connections subjected to Seismic Lateral Loading	Nov. 2009
021	Linderman, L.E., Rice, J.A., Barot, S., Spencer, B.F., and Bernhard, J.T.	Characterization of Wireless Smart Sensor Performance	Feb. 2010
022	Miller, T.I. and Spencer, B.F.	Solar Energy Harvesting and Software Enhancements for Autonomous Wireless Smart Sensor Networks	March 2010
023	Denavit, M.D. and Hajjar, J.F.	Nonlinear Seismic Analysis of Circular Concrete-Filled Steel Tube Members and Frames	March 2010
024	Spencer, B.F. and Yun, C.-B. (Eds.)	Wireless Sensor Advances and Applications for Civil Infrastructure Monitoring	June 2010
025	Eatherton, M.R. and Hajjar, J.F.	Large-Scale Cyclic and Hybrid Simulation Testing and Development of a Controlled-Rocking Steel Building System with Replaceable Fuses	Sept. 2010
026	Hall, K., Eatherton, M.R., and Hajjar, J.F.	Nonlinear Behavior of Controlled Rocking Steel-Framed Building Systems with Replaceable Energy Dissipating Fuses	Oct. 2010